The Risk and Return of Equity and Credit Index Options

Hitesh Doshi, Jan Ericsson, Mathieu Fournier, and Sang Byung Seo[†]

March 15, 2023

Abstract

We estimate a structural model of equity and credit options using data on index default swap and physical equity index volatility. The model predicts reasonable time-series of level, skew, and term-structure of equity- and credit-index implied volatilities out-of-sample. Furthermore, the model predictions for option expected returns closely match empirical estimates. Decomposing returns into asset, variance, and jump risks, we study the sources of risk-return compensation in both derivative markets. Credit-index option expected returns are higher in absolute terms and depend more on variance risk than their equity counterparts which are primarily impacted by systematic asset and jump risks.

JEL classification: G12, G13

---

[*]We thank participants at the Tsinghua Finance Workshop 2019, McGill University brown bag 2019, Tremblant Workshop 2020, ITAM/HEC Montreal Cancun Derivatives Workshop 2020, and the Virtual Derivatives Workshop 2021. In particular, we are grateful to Patrick Augustin, Christian Dorion, Bjørn Eraker, Zhiguo He (discussant), Kris Jacobs, Mete Kilic, Philippe Mueller, Chay Ornthanalai, Nick Pan, Neil Pearson, Ivan Shaliastovich, and Aurelio Vasquez for helpful comments.

[†]Doshi is with the Bauer College of Business at the Univeristy of Houston, Seo is with the University of Wisconsin - Madison, Fournier is with UNSW Business School, while Ericsson is with McGill University. Corresponding author: Jan Ericsson (jan.ericsson@mcgill.ca), Desautels Faculty of Management at McGill University.

1 Introduction

Option returns have been a matter of debate for the last two decades. There are (at least) two facets to this discussion. The first relates to the magnitude of returns: are high returns evidence of mispricing? Another side of the debate relates to the sources of high option returns: what additional sources of risk drive their magnitude? We seek to broaden this discussion by asking whether option prices and expected returns across multiple index derivatives and underlying markets can be jointly reconciled within a structural option pricing model, while also attributing returns to the relevant sources of risk.

A starting point for the debate can be found in the S&P 500 (SPX) option literature with Bondarenko (2014), who documents strikingly high returns to writing put options and argues that these indicate mispricing.[1] Subsequent work by Broadie, Chernov, and Johannes (2009) calls into question the interpretation that options are mispriced on the basis of these high returns and highlight the importance of jump and volatility risk premia. Building on Broadie, Chernov, and Johannes (2009), Chambers, Foy, Liebner, and Lu (2014) argue, in the same setting but with a longer sample, that put returns are too low to be explained by standard option pricing models after all.[2] On top of the seemingly conflicting results on SPX option returns, which has been the primary focus of the literature to date, our knowledge about the prices and returns in other derivative markets and their consistency across markets is still very limited.[3]

Our contribution is to revisit both the question of mispricing and the sources of expected

[1] An earlier important paper is Coval and Shumway (2001) who study option returns and conclude that additional risk factors such as variance risk are likely required to explain their levels.

[2] Other contributions to the broader option returns literature include Israelov and Kelly (2017) who document that state-of-the-art affine pricing models produce counterfactual expected return predictions. Goyal and Saretto (2022) use a reduced form statistical factor model to conclude that options strategies predicated on mispricing do not seem eo generate abnormal returns.

[3] For seminal contributions on derivative prices and returns in other markets, see Cheng (2018) and Eraker and Wu (2017), who study VIX futures. Another notable exception is Collin-Dufresne, Junge, and Trolle (2021) who analyze the pricing consistency of S&P 500 equity and CDX credit options in part by considering returns. Carr and Wu (2011) study the link between credit default swaps and out-of-the money put prices. Culp, Nozawa, and Veronesi (2018) investigate the relation between index put options, treasuries, and corporate bond credit spreads.

return in two derivative markets simultaneously - those for SPX index options and CDX credit index options. Studying these two markets simultaneously is important for two reasons. First, it allows us to contribute to the extant literature on the SPX options market which, while abundant, still lacks a consensus on these questions. Second, we provide new findings for the CDX market where evidence on option prices is scarce and that on returns virtually non-existent.[4] Studying the link between these two markets is particularly important given recent evidence in Collin-Dufresne, Junge, and Trolle (2021) who find that SPX and CDX option prices are hard to reconcile. This result is striking given a significant body of work suggesting a close link between various other credit instruments and equity options.[5]

Figure 1 summarizes our main finding. It shows that our model does a very good job at predicting the cross-section of average historical excess return of the two underlying indices and their derivatives. This is particularly striking given that the model is estimated without using any option price data, and our sample include two crisis periods. Yet, the model is able to match observed patterns in excess returns fairly closely out-of-sample in the two option markets and across contracts.

In order to produce our results, we evaluate a structural credit and equity option pricing model which jointly and consistently links equity and credit index prices via the unlevered asset return and variance dynamics of their constituents. It also endogenously relates prices and returns on equity and credit indices with those on their options. The model allows firms' unlevered assets to exhibit priced common jumps and stochastic volatility. Our estimation uses as inputs credit index term structures and physical equity index volatility. The model fits both of these very well in-sample.[6] Given the estimated parameters and filtered state variables, we obtain time series of predicted implied volatility surfaces for equity and credit options contemporaneously out-of-sample. Our

[4]One exception is Collin-Dufresne, Junge, and Trolle (2021) who provide evidence on the magnitude of straddle returns in equity and credit index markets.

[5]See, among others, Cremers, Driessen, and Maenhout (2008), Culp, Nozawa, and Veronesi (2018), Carr and Wu (2011), Collin Dufresne, Goldstein, and Yang (2012), and Cao, Goyal, Xiao, and Zhan (2022).

[6]By construction, SPX return volatility and 5-year CDX spread are taken to be observed without error. For the other CDX tenors, the errors are about 10-15% of the spread.

Figure 1: Historical Average and Model Expected Excess Returns: Indices and Options

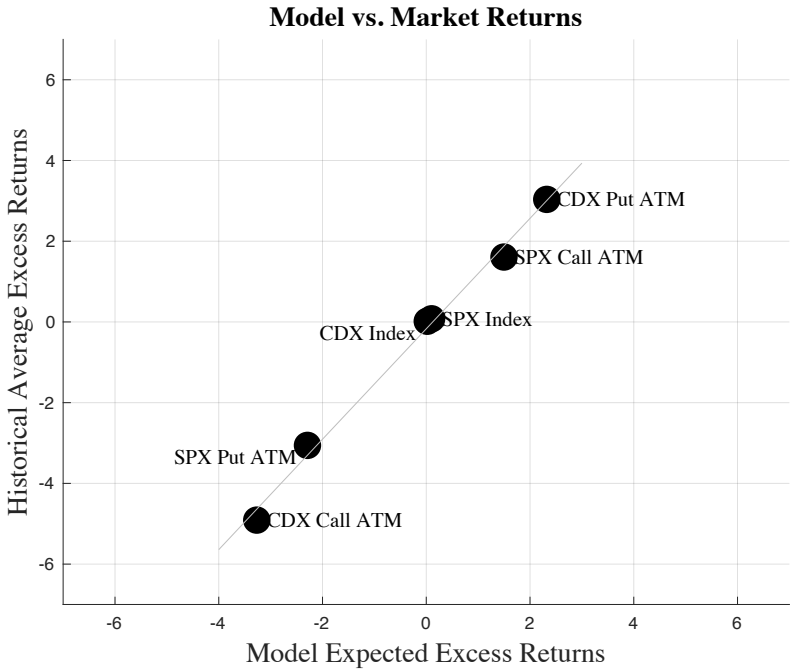

Notes: This figure presents the scatter plot of the model-implied returns versus their empirical counterparts. The empirical market returns are computed as the average return for each index and option during our sample. The sample period is from June 2004 to December for S&P 500 index and its options. The sample period for CDX index and its options is from March 2012 to December 2020. For each of the options, we compute the returns of at-the-money contracts. The CDX index returns are for the five-year maturity CDX index.

model then allows us to compute expected measures of risk and return for underlyings and options in both markets. The structural nature of our framework also provides us with a decomposition of model-predicted returns into components that relate to unlevered market risk, in addition to systematic variance and jump risks.

We first assess our model's ability to predict levels and time series of option prices in the two markets. We do so without resorting to options data in the estimation, and find that implied volatilities for both credit and equity index options are jointly well explained by our model across most levels of moneyness and time to maturity.

Consider SPX options first. The model's performance in predicting average at-the-money implied volatility term structures is good overall, with a slight underestimation for one month out-of-the-money put options. For one, three and six months to expiration, average market (model) at-the-money implied volatilities are respectively 17.0% (16%), 17.2% (17.1%) and 18.3% (17.5%). The model also correctly predicts the average slope of the term structure of implied volatilities being downward sloping for out-of-the money options and upward sloping for others. In the moneyness spectrum, model implied volatility skews replicate observed smiles accurately, particularly so for three and six months to maturity options. In the time-series, the correlations between data and model implied volatilities are higher than 80% across the board.[7]

When it comes to CDX options, the ability to explain skews and term structures of implied volatilities out-of-sample is qualitatively and quantitatively similar to the equity index option case. For one, three and six months to expiration, average market (model) at-the-money implied volatilities are respectively 45.2% (47.3%), 47.1% (49.3%), and 49.4% (46.7%). Note that for the CDX options, term structures are on average positively sloped regardless of moneyness, in fact steeper for out-of-the-money options. The time series correlations for CDX options are slightly lower than for SPX options (correlations are 77%, 71%, and 56% respectively for one, three and six month at-the-money implied volatilities). This small difference compared to the SPX option

[7]This performance is not merely an artefact of having fitted the physical volatility perfectly. The correlation between data and model volatility premia are in the range of 55 % to 80% depending on option expirations.

fit is to be expected as credit spread index volatility is not an input to the estimation whereas the physical equity index volatility is.

To produce expected return predictions, information about physical and risk-neutral dynamics is required to back out risk premium estimates which, combined with exposures, define return compensations. In addition to fitting CDX index prices across tenors and time, our model is tasked with matching the level and time series of the physical volatility of the SPX index. Combined, these data allow us to identify both model physical and risk-neutral dynamics. To gauge the reasonableness of estimated parameters over and beyond pricing performance, we also consider physical quantities such as cumulative default probabilities, leverage ratios, and asset Sharpe ratios. Overall, we find that the model matches these metrics well.[8]

Given these encouraging findings, we then proceed to examine average option excess returns, as well as those for their underlyings. Echoing Broadie, Chernov, and Johannes (2009), we find that realized SPX option returns, while high, do not appear to suggest any mispricing - average realized excess returns line up well with model predicted return levels, as illustrated in Figure 1. A key novel contribution we make is to show that this is also true for credit index options, whose realized and predicted returns are higher in absolute terms than those of SPX options. For example, SPX puts returned on average -256% per annum while the economically similar CDX calls returned -438%. The model predicted returns for the two contracts are -223% and -374%, respectively.

An advantage of a using a structural model is that the indices that underlie both types of options are themselves contingent claims. For example, CDX index prices are, just like CDX options, contingent claims on the assets of the constituent firms. Hence using the time series of credit index spreads in the estimation is informative not just about physical dynamics but also risk-neutral asset dynamics. This allows us to estimate our model without using any option information

[8]The model-implied 10-year cumulative physical default probability is 2.57%, which is close to the 10-year default rate of 2.29% for investment grade entities reported in Moody's credit report for the 1998-2018 period. The market leverage of the representative firm implied by the model is 46.11% which is comparable to the 49% average market leverage of firms that belong to both the SPX and CDX indices as measured by the ratio of total liabilities, Compustat item LTQ, to market equity plus total liabilities.

and study the two derivative markets simultaneously out-of-sample. Pricing options out-of-sample would be much more difficult, if not impossible, in a standard reduced form model where underlying index return dynamics are specified exogenously. This is because return realizations are only informative about the physical probability measure and thus the use of option information is required to estimate risk-neutral dynamics. In addition, the reduced form nature of these models makes it more difficult to consistently link multiple derivative markets jointly. In sum, working with a structural model permits a more stringent economic validation, (i) by benchmarking with physical quantities and (ii) by allowing cross-market comparisons.

Another key feature of our model is to allow the decomposition of returns based on the three sources of systematic risk driving asset dynamics: unlevered asset risk, variance risk and jump risk. Predicting expected returns for options across two different markets jointly and out-of-sample, is clearly more difficult than for one, unless the two markets are similar in terms of risk exposures and are effectively substitutes. We show that this is not the case and that the two indices and their option markets differ significantly in their underlying risk exposures, both qualitatively and quantitatively.

Both indices load positively on asset risk and, as expected, the equity index has a much larger exposure. The equity index has a positive exposure to variance risk, consistent with the Merton (1974) intuition that stocks can be viewed as calls on firm's assets. However, this exposure is relatively small in magnitude. The credit index on the other hand, loads heavily on this risk, consistent with bondholders seen as selling puts on firms' assets. While jump risk impacts both indices, the equity index is more exposed to tail events.

Moving on to options, SPX at-the-money calls (puts) derive a positive (negative) risk premium from asset risk and jump risk. A credit index call option is economically similar to an equity put - both pay off in adverse states of the world. As a result, CDX option returns have qualitatively similar elasticities to asset and jump risk, but with opposite sign to that of SPX options. For instance, CDX calls require a lower return premium due to jumps.

In a compound pricing framework such as ours, the fact that the underlying itself is a contingent

claim implies that put-call parity does not imply that vegas of calls and puts with the same strike price and expiration must be equal, or even of the same sign. This is because the underlying is also exposed to variance risk. Regarding SPX options, we find that both at-the-money calls and puts have comparable positive variance elasticities. This result is explained by the fact that their underlying index is only marginally exposed to variance. Contrary to the equity index option case, CDX calls and puts have opposite exposures on variance risk where calls are positively exposed but puts negatively. As the underlying credit index spread is strongly increasing in variance, it reinforces the positive exposure of call options but offsets that of put options, resulting in negative CDX put vegas.

The literature on the impact of variance risk on SPX option returns is large but disagrees on its economic magnitude. For instance, Coval and Shumway (2001) suggest that systematic variance is key to explain SPX option returns. However, Pan (2002) and Broadie, Chernov, and Johannes (2009) argue that variance risk cannot be a significant contributor to SPX option prices because these options are short-term in nature, which does not leave enough time for this source of risk to materially impact their prices.

Although we find that SPX option returns do load on variance risk, their exposure to variance is about 3 times smaller than that of credit options. This result calls to mind the finding in Du, Elkamhi, and Ericsson (2019) who find that accounting for variance risk in a structural credit model is important to explain corporate bond credit spreads. The fact that variance risk matters more for CDX options than for SPX options can be rationalized by the fact that the underlying CDX is itself heavily exposed to variance risk. Because of the compounding effect of embedded leverage, credit option prices, in particular CDX calls, become significantly influenced by variance risk. While about 20% of at-the-money SPX put option expected return is attributable to systematic variance exposure, 56% of CDX call expected returns is derived from exposure to aggregate volatility. Overall, we find that SPX options offer more embedded leverage to asset and jump risks but that trading CDX options offers more exposure to aggregate variance risk.

Our work is related to several strands of literature. The first consists of recent work that links

credit and equity derivative markets. Cremers, Driessen, and Maenhout (2008) use equity index and option prices to imply jump risk premia in order to predict credit spreads. Collin-Dufresne, Goldstein, and Yang (2012) use a model fitted to long-dated equity index options and CDX index term structures to value tranches of collateralized debt obligations out-of-sample. Culp, Nozawa, and Veronesi (2018) use index option prices to imply credit spreads in a model-free setting. All of these papers have in common that they price corporate credit instruments out-of-sample using a model estimated on data from other markets. There are at least three key differences between previous works and ours. First, our estimation works in a different direction in the sense that we use data on credit spreads (CDX term structures), together with physical equity index volatility, to obtain out-of-sample predictions for options. Second, we link four markets consistently, the SPX and CDX markets together with their corresponding derivatives. Finally, our primary focus is on expected option returns which have received less attention. Like much of previous work, we find that the four markets are closely related.

One closely related paper is Collin-Dufresne, Junge, and Trolle (2021) who also study the markets for credit and equity index options and document difficulty in reconciling the prices in the two derivatives markets, interpreting their findings as a lack of integration. However, we find no evidence of a lack integration between the two markets, nor any systematic mispricing.

We investigate whether the differences in results can be explained by differences in model setup and conclude that this is not the case.[9]

Another literature studies the magnitude and properties of variance, jump, and tail risk premia in financial securities.[10] Most existing work in this literature focuses on equity index and index option markets. Our contribution is to broaden the study of variance and jump risk premia to

[9]In Appendix D, we replicate Collin-Dufresne, Junge, and Trolle (2021)'s main result in our model using their parameter sets. The differences in parameters could arise from differences in estimation procedure - we estimate the model fully in sample by maximum likelihood, whereas they recalibrate their model at distinct dates. Their parameters generate risk-neutral distribution for credit index spreads that much more kurtosis than ours.

[10]For seminal contributions in this literature, see, among others, Bates (2000), Pan (2002), Eraker, Johannes, and Polson (2003), Carr and Wu (2009a), Todorov (2010a), Andersen, Fusari, and Todorov (2020), and Andersen, Todorov, and Ubukata (2020).

multiple markets simultaneously and to trace back the sources of risk premia in these markets to those of the underlying asset of the firm.

The outline of the rest of the paper is as follows. The next section describes our model. In section 3.1 we describe our data and estimation approach. Section 4 reports on our model validation, in-sample on CDX terms structures and out-of-sample on equity and credit option price levels. It also contains a discussion of our main results on option returns. Section 6 concludes.

2 Model

In this section, we develop a structural credit risk model which allows us to consistently price equity, credit, and associated derivative contracts from the ground up. First, we introduce the asset dynamics for individual firms and the economy's stochastic discount factor (Section 2.1). Based on the specified dynamics, we derive firm-specific asset risk-neutral dynamics and unlevered asset risk premia (Section 2.2). The pricing of a credit default swap (CDS) is discussed in Section 2.3. We then construct the equity and credit indices and calculate prices for their option contracts in Section 2.4. Given our pricing results, we derive a decomposition of risk premia and variances for our indices and index options in Section 2.5. Using this result, we then study the relative contributions of the various sources of uncertainty to expected returns and volatility risk premia across four different markets.

2.1 Asset Value and Variance Dynamics

We consider a cross-section of firms $j \in [1, \ldots, N]$ whose return dynamics under the physical probability measure $\mathbb{P}$ are driven by the systematic asset factor A_t^m as well as two types of idiosyncratic shocks:

$$\frac{dA_t^j}{A_t^j} = \frac{dA_t^m}{A_t^m} + \sigma_j dW_t^j + dJ_t^j - \lambda^j \bar{\nu}^j dt, \tag{1}$$

where dW_t^j is a standard Brownian motion and $dJ_t^j = \tilde{\nu}_t^j dN_t^j$ is a jump process capturing idiosyncratic variation in firm j's unlevered asset value, A_t^j. The jump intensity is $\mathbb{E}_t\left[dN_t^j\right] = \lambda^j dt$, where $\mathbb{E}_t\left[\cdot\right]$ denotes a time-t conditional physical expectation.[11] Conditional on the occurrence of an idiosyncratic jump at time t, counted by the Poisson process dN_t^j, the change in asset value caused by an idiosyncratic jump is $A_t^j \tilde{\nu}_t^j$, where the multiplicative jump size is $\tilde{\nu}_t^j \equiv (e^{\tilde{Z}_t^j} - 1)$. The jump size variable $\tilde{Z}_t^j$ is assumed to be normally distributed with time-invariant parameters such that $\tilde{Z}_t^j \sim N(z_j, \gamma_j^2)$. Note that we use tilde superscripts to indicate that both $\tilde{\nu}_t^j$ and $\tilde{Z}_t^j$ are random as of time t.[12] The expected idiosyncratic jump size is denoted by $\bar{\nu}^j = \mathbb{E}_t\left[\tilde{\nu}_t^j\right]$.

While both types of idiosyncratic shocks are i.i.d. with constant volatility (σ_j) and jump intensity (λ^j), we assume that the systematic component features stochastic volatility.[13] As in Du, Elkamhi, and Ericsson (2019), under the physical measure $\mathbb{P}$, the dynamics of the aggregate asset component, A_t^m, and its stochastic variance, V_t, are characterized by the following stochastic differential equations under $\mathbb{P}$:

$$\frac{dA_t^m}{A_t^m} = (\mu_t - q)\, dt + \sqrt{V_t} dW_t^A + dJ_t^m - \lambda_t^m \bar{\nu}^m dt, \tag{2}$$

$$dV_t = \kappa(\theta - V_t)dt + \delta\sqrt{V_t} dW_t^V, \tag{3}$$

where μ_t is the expected return on the unlevered "market" and q is the payout rate.[14] The systematic variance V_t follows a square-root process where κ, θ, and δ represent the mean-reversion

[11] The filtration at any time corresponds to the information set associated with knowing all realizations of uncertainty in our model up to that point in time.

[12] For ease of exposition, we do not differentiate the time right before or right after a jump which are usually denoted by t_- and t_+ in the literature. Instead, we use the simplified notation $\tilde{\nu}_t^j$ (or $\tilde{Z}_t^j$) to denote the random multiplicative jump (or the random jump size) in asset caused by an idiosyncratic jump that would have incurred at time t.

[13] It is straightforward to allow for stochastic idiosyncratic volatility or stochastic idiosyncratic jump intensity. However, this would increase the complexity of the estimation strategy by adding more state variables to filter over time and more structural parameters to estimate. To maintain parsimony, we assume constant volatility and constant jump intensity for the idiosyncratic component.

[14] Note that we assume the same payout rate for all firms. As a result, incorporating the payout rate in individual firm asset dynamics or in the common asset factor is equivalent.

speed, long-run mean, and volatility of volatility parameters, respectively. To model correlation between asset value and variance shocks, we assume that $dW_t^A = \rho dW_t^V + \sqrt{1-\rho^2} dW_t^{A\perp V}$ where dW_t^V and $dW_t^{A\perp V}$ are two mutually independent Brownian motions. When $\rho < 0$, aggregate asset variance is high when the level of aggregate assets is low. This case implies a negative skewness in the distribution of unlevered market returns, consistent with empirical evidence.[15]

In addition to systematic diffusive risk, we allow for systematic jumps captured by the jump process $dJ_t^m = \tilde{\nu}_t^m dN_t^m$, where dN_t^m is another Poisson process, counting the occurrence of systematic jumps with time-varying $\mathbb{P}$-intensity $\mathbb{E}_t\left[dN_t^m\right] \equiv \lambda_t^m dt = \eta_m V_t dt$.[16] In our model, the systematic jump intensity is proportional to systematic asset variance and will be higher in bad times when systematic variance is higher. Conditional on a jump at time t, the change in aggregate asset value is $A_t^m \tilde{\nu}_t^m$, where $\tilde{\nu}_t^m \equiv (e^{\tilde{Z}_t^m} - 1)$ with $\tilde{Z}_t^m \sim N(z_m, \gamma_m^2)$ under $\mathbb{P}$. The expected proportional systematic jump size is denoted by $\bar{\nu}^m = \mathbb{E}_t\left[\tilde{\nu}_t^m\right]$.[17]

The economy is endowed with a stochastic discount factor (SDF) used to price firms' financial claims. Following the literature on variance and jump risks, we assume that the SDF is exponentially affine in aggregate risks. We have

$$\frac{d\phi_t}{\phi_t} = -rdt - \xi_{A\perp V}\sqrt{V_t} dW_t^{A\perp V} - \xi_V \sqrt{V_t} dW_t^V + \left(e^{\xi_m \tilde{Z}_t^m} - 1\right) dN_t^m, \tag{4}$$

where $\xi_{A\perp V}$, ξ_V, and ξ_m are the market price of risk parameters for unlevered asset level diffusive risk, variance risk, as well as systematic jump risk, respectively. Note that firms' idiosyncratic risks are deliberately not priced in the model.

[15]For discussions on the presence of negative skewness in the distribution of systematic risks, see Berger, Dew-Becker, and Giglio (2020), among others.

[16]this is the same specification used in Pan (2002).

[17]Again, we use the simplified notation $\tilde{\nu}_t^m$ (or $\tilde{Z}_t^m$) to denote the random multiplicative jump (or the random jump size) in asset caused by a systematic jump taking place at time t. Thus, $\tilde{\nu}_t^m$ and $\tilde{Z}_t^m$ are both random as of time t.

2.2 Risk-Neutral Dynamics and Unlevered Asset Risk-Premia

The above SDF, combined with asset return and variance dynamics, have direct implications for the economy risk-neutral ($\mathbb{Q}$) dynamics and the risk-premia of systematic asset return and variance risks. More precisely, the risk-neutral dynamics of A_t^m and V_t can be expressed as:

$$\frac{dA_t^m}{A_t^m} = (r-q)\,dt + \sqrt{V_t}dW_t^{A,\mathbb{Q}} + dJ_t^{m,\mathbb{Q}} - \lambda_t^m \bar{\nu}^m dt, \tag{5}$$

$$dV_t = \kappa^{\mathbb{Q}}(\theta^{\mathbb{Q}} - V_t)dt + \sigma\sqrt{V_t}dW_t^{V,\mathbb{Q}}, \tag{6}$$

where $dW_t^{A,\mathbb{Q}} = \rho dW_t^{V,\mathbb{Q}} + \sqrt{1-\rho^2}dW_t^{A\perp V,\mathbb{Q}}$, $\kappa^{\mathbb{Q}} = \kappa + \delta\xi_V$ and $\theta^{\mathbb{Q}} = \kappa\theta/\kappa^{\mathbb{Q}}$. A superscript $\mathbb{Q}$ is used to identify risk-neutral parameters, Brownian motions, and jumps implied by the SDF.[18] When systematic jump risk is priced, it simultaneously shifts the risk-neutral jump intensity and the mean of systematic jumps. We have $dJ_t^{m,\mathbb{Q}} = \tilde{\nu}_t^{m,\mathbb{Q}} dN_t^{m,\mathbb{Q}}$ with $\mathbb{E}_t^{\mathbb{Q}}\left[dN_t^{m,\mathbb{Q}}\right] = \lambda_t^{m,\mathbb{Q}}dt = \lambda_t^m e^{\xi_m z^m + \frac{1}{2}(\xi_m)^2\gamma_m^2}dt$ and $\tilde{\nu}_t^{m,\mathbb{Q}} = (e^{\tilde{Z}_t^{m,\mathbb{Q}}} - 1)$ with $\tilde{Z}_t^{m,\mathbb{Q}} \sim N(z_m^{\mathbb{Q}}, \gamma_m^2)$ for which $z_m^{\mathbb{Q}} = z_m + \xi_m\gamma_m^2$. Given that idiosyncratic risk is not priced in our model, the risk-neutral dynamics of A_t^j can be derived by inserting equations (5) and (6) into equation (1).

In the absence of arbitrage opportunities, the (instantaneous) asset risk premium, which is the difference between the expected asset return μ_t and the risk-free rate r, is given by

$$(\mu_t - r)\,dt = \left((\sqrt{1-\rho^2}\xi_{A\perp V} + \rho\xi_V)V_t\right)dt + \left(\lambda_t^m \mathbb{E}_t\left[\tilde{\nu}_t^m\right]dt - \lambda_t^{m,\mathbb{Q}}\mathbb{E}_t^{\mathbb{Q}}\left[\tilde{\nu}_t^{m,\mathbb{Q}}\right]\right)dt, \tag{7}$$

where the first term captures the compensation for diffusive asset return and variance risks, while the second corresponds to the asset jump risk premium.[19]

[18] Applying Girsanov's theorem, we have $dW_t^{A\perp V} = dW_t^{A\perp V,\mathbb{Q}} - \xi_{A\perp V}\sqrt{V_t}dt$ and $dW_t^V = dW_t^{V,\mathbb{Q}} - \xi_V\sqrt{V_t}dt$.

[19] Note that $\mathbb{E}_t[\tilde{\nu}_t^m] = e^{(z_m)^2 + \frac{1}{2}(\gamma_m)^2} - 1$ and $\mathbb{E}_t^{\mathbb{Q}}[\tilde{\nu}_t^{m,\mathbb{Q}}] = e^{(z_m^{\mathbb{Q}})^2 + \frac{1}{2}(\gamma_m)^2} - 1$, respectively.

2.3 The Pricing of Firms' Equity and Credit Securities

Following Leland (1994), we assume that each firm issues consol bonds. Firm j declares bankruptcy when the firm's asset value falls below a certain threshold A_D. In other words, the timing of the firm's default, τ_j, is modeled as the first time at which the asset value A_t^j in equation (1) hits the default boundary A_D:

$$\tau_j = \inf\{s \geqslant t | A_s^j = A_D\}.$$

Prices of a firm's securities and contingent claims in the model derive from the risk-neutral distribution of τ_j and are a function of two key quantities: (i) the present value of a dollar received at default $P_D(A_t^j, V_t) = \mathbb{E}_t^{\mathbb{Q}}\left[e^{-r(\tau_j - t)}\right]$, and (ii) the cumulative risk-neutral default probability $G(A_t^j, V_t, T) = \mathbb{E}_t^{\mathbb{Q}}\left[\mathbb{1}_{\tau_j \leqslant T}\right]$ over the next T years. Equipped with these measures, we are able to price any security issued by the firm as well as associated derivative contracts. Appendix C.2 contains the details about the estimation of $P_D(A_t^j, V_t)$ and $G(A_t^j, V_t, T)$ for a given set of structural parameters in our set-up.[20]

To begin, we calculate the firm's debt value $D(A_t^j, V_t)$ as the present value of future coupon payments plus the recovery value of the firm upon default:

$$D(A_t^j, V_t) = \frac{c}{r} + \left[(1-\alpha)A_D - \frac{c}{r}\right] P_D(A_t^j, V_t), \tag{8}$$

where c is the coupon rate and α is the liquidation cost. For simplicity, we assume that firms have the same coupon, liquidation cost, default barrier, and idiosyncratic diffusive and jump parameters. With leverage, the firm value can deviate from its unlevered counterpart A_t^j due to two reasons. First, the firm can enjoy tax benefits arising from the firm's debt. If the tax rate is ζ (for all firms), the present value of future tax shields is $\frac{\zeta c}{r}\left[1 - P_D(A_t^j, V_t)\right]$. However, this benefit comes with a cost. The debt exposes the firm to the risk of default, at which point it will incur

[20] More precisely, our estimation strategy builds on Du, Elkamhi, and Ericsson (2019) who develop a simulation approach to obtain the (smooth) mapping between $P_D(\cdot)$ and $G(\cdot, T)$ and a given pair of state variables (A_t^j, V_t) using two-dimensional Chebyshev polynomials.

financial distress costs. The present value of future bankruptcy costs is $\alpha A_D P_D(A_t^j, V_t)$. Hence, the levered firm value is given by

$$L(A_t^j, V_t) = A_t^j + \frac{\zeta c}{r}\left[1 - P_D(A_t^j, V_t)\right] - \alpha A_D P_D(A_t^j, V_t). \tag{9}$$

Since the firm's equity is a residual claim, its value is calculated as the difference between the levered firm value and the debt value, $L(A_t^j, V_t) - D(A_t^j, V_t)$. It is given by

$$E(A_t^j, V_t) = A_t^j - \frac{(1-\zeta)c}{r} + \left[(1-\zeta)\frac{c}{r} - A_D\right] P_D(A_t^j, V_t). \tag{10}$$

Lastly, we consider the pricing of a CDS contract, which insures against the firm's potential default in the future. A CDS contract involves two parties: the protection buyer and the protection seller. The protection buyer makes quarterly premium payments to the protection seller until the maturity of the contract or until the firm's default. Economically, in the event of a default, the protection seller has an obligation to buy the defaulted bond at par from the protection buyer, thus absorbing the default loss. In practice, this settlement is often done instead as a cash payment based on a post default market value determined by a third party.

When the running spread paid by the protection buyer is one basis point (bp) per annum, the present value of future premiums (or premium leg) is called the risky PV01, or RPV01(A_t^j, V_t, T). If the running spread is, for example, 100 bp, the premium leg is simply obtained as $100 \times$ RPV01. In exchange for paying insurance premiums, the protection buyer acquires a contingent claim which makes up the loss on the firm's bonds in the event of a default. We denote the present value of a contingent protection payment (or protection leg), ProtLeg(A_t^j, V_t, T). We refer the reader to Appendix A.1 for details about the computation of RPV01$(\cdot)$ and ProtLeg$(\cdot)$. By definition, a CDS spread S refers to the fair market spread that equates the premium leg ($S \times$ RPV01) with the protection leg (ProtLeg). We have:

$$S(A_t^j, V_t, T) = \frac{\text{ProtLeg}(A_t^j, V_t, T)}{\text{RPV01}(A_t^j, V_t, T)}. \tag{11}$$

2.4 Indices and their Options

So far, we have defined the dynamics of the underlying unlevered firm asset value and described the valuation of corporate securities as well as credit default swaps. Ultimately, our goal is to value equity and credit indices, as well as options on such indices. To this end, we first define the value of an equally-weighted index. We then consider the resulting index dynamics and how they can be used to study the S&P 500 index (in short, SPX), the CDX North American Investment Grade Index (in short, CDX), and their options.

Consider an equally weighted index with N constituents, $I_t \equiv I(A_t^1, \ldots, A_t^N, V_t)$, defined as

$$I_t \;=\; \frac{1}{N}\sum_{j=1}^{N} f(A_t^j, V_t),$$

where f can be firm j's stock price, CDS spread, or any other claim written on its assets. In our implementation, we consider a cross-section of 500 firms ($N = 500$) representing the SPX.[21] Without any further assumptions, modeling the dynamics of an index composed of 500 firms would require keeping track of 501 state variables over time (i.e., A_t^j for $j = 1, ..., 500$ and V_t).

To alleviate this computational challenge, we follow the literature and approximate the index with a pool of homogeneous ex-ante identical firms (see e.g. Vasicek, 2002; Collin-Dufresne, Goldstein, and Yang, 2012; Seo and Wachter, 2018; Collin-Dufresne, Junge, and Trolle, 2021). We hypothesize that a firm represents the average of the firms in the index and denote this firm by superscript r instead of j, and, like other firms, its asset dynamics are described by equation (1). At each pricing date t, the homogeneity assumption, $A_t^j = A_t^r$ for all $j \in [1, \ldots, N]$, implies that the index satisfies $I_t = \frac{1}{N}\sum_{j=1}^{N} f(A_t^r, V_t) = f(A_t^r, V_t)$. This leaves us with only two state variables to model: the representative asset value, A_t^r, and the common factor variance, V_t. It is important

[21] We make an implicit assumption that the equity index and the credit index are both based on the same pool of underlying firms. This is not exactly the case in practice as the SPX consists of 500 firms while the CDX is composed of 125 firms. However, Collin-Dufresne, Junge, and Trolle (2021) show, by comparing key characteristics such as ratings, leverage, and total/idiosyncratic asset volatility, that modeling the two indices assuming the same number of constituents is relatively innocuous in a setting such as ours.

to note the distinction between levels and dynamics here. The mapping from representative asset value to index value is a function of the dynamics in (1) where $j = r$, however the dynamics of the index will see the idiosyncratic risk diversify away. We refer to Appendix B.2 for details of the dynamics of an index composed of homogeneous firms which assets evolve according to equation (1).

In our empirical analysis below, we use call and put option contracts on the SPX, as well as payer and receiver swaption contracts on the CDX. Calls and puts written on one of these indices, are valued according to

$$c(I_t, K, T) = e^{-rT}\mathbb{E}_t^{\mathbb{Q}}\left[max(I_{t+T} - K, 0)\right], \tag{12}$$

$$p(I_t, K, T) = e^{-rT}\mathbb{E}_t^{\mathbb{Q}}\left[max(K - I_{t+T}, 0)\right]. \tag{13}$$

The constituents f of the index I are thus either the stock prices of the SPX index or the up-front equivalent of the 5 year CDX index.[22] A detail which we consider in Appendix A.2 is that options on the CDX are adjusted for the possiblity that defaults occur in the index prior to the expiration of the option. Appendix B.2 contains the details about index derivative dynamics in our framework.

To calculate option prices, we simulate the risk-neutral asset dynamics of 500 ex-ante homogeneous firms. While all of the firms are given the same initial value ($A_0^j = A_0^r$ for all j), their simulated asset values in the future can deviate from one another due to distinct idiosyncratic shocks (W_t^j and J_t^j). For each simulation path, the index option payoffs at time $t + T$ are determined by the 500 simulated asset values A_{t+T}^j together with the systematic variance component V_t. We repeat this 10,000 times and calculate the conditional expectations in equations (12) and (13) as the averages across 10,000 simulation paths.

Next, we consider excess returns and volatilities of indices and index derivatives, with a view

[22]The distinction between a CDS quoted as a basis point spread and up-front is merely a matter of convention. The CDX tracks an equally-weighted basket of investment-grade single-name CDS contracts. Hence, the quoted up-front fee for the CDX should be identical to the average of the upfront fees for the underlying contracts.

to understanding how the various sources of diffusive and jump risks we model contribute to these moments across the different markets.

2.5 The Sources of Expected Return and Variance Across Markets

The valuation framework we develop allows us to jointly identify how asset risk, variance risk, and jump risk, contribute to (instantaneous) expected returns and volatilities for the securities that we consider in our empirical exercise.

To be more specific, consider a security $g(A_t^r, V_t)$, which could be a tradeable unit of the index, $g = I$ or an option on this index, $g = c$ or $g = p$. Then the following proposition details the sources of its risk premium as a function of its exposures to the various sources of uncertainty impacting the asset dynamics in (1).

Proposition 1. *Consider an index or an index derivative $g \in \{I, c, p\}$. Given the $\mathbb{P}$-dynamics in (1)-(3) combined with the SDF in (4) and the homogeneity assumption above, the instantaneous return risk premium on $g_t \equiv g(A_t^r, V_t)$, $\mathbb{E}_t\left[\frac{dg_t}{g_t}\right] - E_t^{\mathbb{Q}}\left[\frac{dg_t}{g_t}\right]$, is*

$$= \underbrace{\Delta_{A,t}\left(\mu_t - r\right)dt}_{Asset\ risk\ premium} + \underbrace{\Delta_{V,t}\left(\delta\xi_V V_t\right)dt}_{Variance\ risk\ premium} + \underbrace{\left(\mathbb{E}_t\left[\frac{dJ_t^{m,g}}{g_t}\right] - \mathbb{E}_t^{\mathbb{Q}}\left[\frac{dJ_t^{m,g,\mathbb{Q}}}{g_t}\right]\right)}_{Jump\ risk\ premium}, \tag{14}$$

where $\Delta_{A,t} \equiv \frac{\partial g_t}{\partial A_t^r}\frac{A_t^r}{g_t}$, $\Delta_{V,t} \equiv \frac{\partial g_t}{\partial V_t}\frac{1}{g_t}$, $dJ_t^{m,g} \equiv \left(g(A_t^r e^{\tilde{Z}_t^m}, V_t) - g_t\right) dN_t^m$, and $dJ_t^{m,g,\mathbb{Q}} \equiv \left(g(A_t^r e^{\tilde{Z}_t^{m,\mathbb{Q}}}, V_t) - g_t\right) dN_t^{m,\mathbb{Q}}$.

Proof. See Appendix B. □

Proposition 1 provides important insights about the factors that influence expected excess returns and return variances of large diversified indices of corporate contingent claims and options written on such indices. Below, we exploit these relationships to quantify the sources of risk premia and variance in the SPX and CDX indices and their options.

From equation (14), we see that the total expected excess return consists of three terms, each of which corresponds to a given source of systematic risk. The first, $\Delta_{A,t}(\mu_t - r)$, which we label *asset risk premium* corresponds to the part of expected return derived from security g's exposure to fluctuations in asset value. It is the product of security g's sensitivity to changes in the representative firm asset value times g's embedded leverage (i.e, $\Delta_{A,t} = \frac{\partial g_t}{\partial A_t^r}\frac{A_t^r}{g_t}$) multiplied by the unlevered asset risk premium (i.e., $\mu_t - r$). Because $\mu_t - r > 0$, positive exposure to asset risk is compensated by a positive *asset risk premium*.

The second term impacting security g's excess expected return corresponds to the part resulting from its exposure to diffusive variance risk and is accordingly labelled *variance risk premium*. The greater the exposure to aggregate variance risk for a given security g, the greater the proportional impact (in absolute terms) of the variance risk premium on g's total excess expected return. Given that aggregate variance risk is counter-cyclical, we tend to have $\xi_V < 0 \Rightarrow \delta\xi_V V_t < 0$. As a result, a security g positively (negatively) exposed to aggregate variance risk bears a negative (positive) *variance risk premium*.

The third and last term contributing to the total excess return is the *jump risk premium*. This premium consists of the difference between physical and risk-neutral expected return on g induced by systematic jumps. For a given probability measure, it is the expected return that g would experience following a single jump multiplied by the expected jump intensity. Typically, we expect to see that $\mathbb{E}_t\left[\tilde{Z}_t^m\right] > \mathbb{E}_t^{\mathbb{Q}}\left[\tilde{Z}_t^{m,\mathbb{Q}}\right]$ and $\mathbb{E}_t\left[dN_t^m\right] = \lambda_t^m dt < \mathbb{E}_t^{\mathbb{Q}}\left[dN_t^{m,\mathbb{Q}}\right] = \lambda_t^{m,\mathbb{Q}} dt$ for jump intensity. These results imply that the *jump risk premium* is positive for securities whose value increases with unlevered asset value.

The following proposition provides the return variance of an index or index derivative.

Proposition 2. *Consider an index or an index derivative $g \in \{I, c, p\}$. Given the $\mathbb{P}$-dynamics in (1)-(3) combined with the SDF in (4) and the homogeneity assumption above, the instantaneous*

$\mathbb{P}$-*variance of the returns on* $g_t = g(A_t^r, V_t)$, $\sigma_{g,t}^2 \equiv var\left(\frac{dg_t}{g_t}\right)$, *is given by*

$$= \underbrace{(\Delta_{A,t})^2 var\left(\frac{dA_t^m}{A_t^m}\right)}_{Asset\,risk} + \underbrace{(\Delta_{V,t})^2 var\,(dV_t)}_{Variance\,risk} + \underbrace{2\,(\Delta_{A,t}\Delta_{V,t})\,cov\left(\frac{dg_t}{g_t}; dV_t\right)}_{Leverage\,risk} + \underbrace{var\left(\frac{dJ_t^{m,g}}{g_t}\right)}_{Jump\,risk}$$

$$= \left(\underbrace{(\Delta_{A,t})^2 V_t}_{Asset\,risk} + \underbrace{(\Delta_{V,t})^2 V_t}_{Variance\,risk} + \underbrace{2\rho\delta\,(\Delta_{A,t}\Delta_{V,t})\,V_t}_{Leverage\,risk} + \underbrace{\lambda_t^m \mathbb{E}_t\left[\frac{g(A_t^r e^{\tilde{Z}_t^m}, V_t)}{g_t} - 1\right]^2}_{Jump\,risk} \right) dt \tag{15}$$

where $\Delta_{A,t}$, $\Delta_{V,t}$, $dJ_t^{m,g}$, *and* $dJ_t^{m,g,\mathbb{Q}}$ *are as defined in Proposition 1.*

Proof. See Appendix B. □

We now turn to the empirical analysis.

3 Data and Estimation

We first discuss the data used and then present our estimation strategy. Results on model fit are discussed in the subsequent sections.

3.1 Data

Our empirical analysis relies on four different data sets. The model estimation is based on the daily time series of the following five variables: the CDX spreads with 3-, 5-, 7-, and 10-year maturities and the physical SPX volatility.[23] The data on the CDX are obtained from Markit. The physical (conditional) volatilities of the SPX are estimated by fitting an NGARCH model with a skewed student t-distribution to daily SPX returns. The daily time series of the SPX are from the CRSP dataset. For estimation purposes, our sample period begins in June 2004, from which the CDX data become available, and ends in December 2020.

[23]The CDX (credit default swap index) is an index composed of 125 individual CDS of investment grade bonds.

We also collect monthly pricing data on SPX options and CDX swaptions (options on the CDX spread). These data serve two purposes. They are used to conduct an out-of-sample analysis of model performance and to study the relative pricing of diffusive and tail risk in the returns of different derivatives. First, we download SPX option prices from OptionMetrics. For a given trading day, we convert SPX option prices into Black-Scholes-implied volatilities and construct the volatility surface via polynomial interpolation. Then, we select the implied volatilities at 95%, 100%, and 105% moneyness values for 1-, 3-, and 6-month maturities. The sample period for SPX options spans the same period covered by our estimation and begins in June 2004 and ends in December 2020. Second, we obtain CDX swaption quotes from a major investment bank. CDX swaptions in our data are based on the 5-year CDX and trade with 1-, 3-, and 6-month maturities. These options are quoted in terms of Black-implied volatilities, and we choose the implied volatilities whose strike upfront fees correspond to 95%, 100%, and 105% of the current CDX spread. The sample period for CDX swaptions starts relatively late, from March 2012. These option contracts trade with meaningful volumes and liquidity since 2012.

3.2 Estimation Strategy

In total, the model features 21 structural parameters and 2 latent variables. The starting point of our estimation strategy thus consists of reducing the dimensionality of the problem by fixing the values of some parameters following Du, Elkamhi, and Ericsson (2019) and Feldhütter and Schaefer (2018), among others. More precisely, we set the bankruptcy cost α to 25%, corporate tax rate ζ to 20%, and CDS/bond-specific recovery rate R to 51% when computing the protection leg of the CDS (see Appendix A.1). Considering our sample period, we choose the risk-free rate to be 1% and the asset payout ratio to be 2%. We set the amount of book debt to 25. Consequently, the coupon payment c is determined as $r \times 25 = 0.25$. The default boundary A_D is set to be 78% of the book debt, which is 19.50.[24] After imposing these 7 identification restrictions, 14 structural parameters remain to be estimated.

[24]This number is broadly consistent with the estimates in Davydenko (2012).

To further reduce the estimation dimensionality, we fix the idiosyncratic jump intensity λ_j at 0.5%, as simultaneously identifying the jump intensity and the jump size distribution is often challenging.[25] This idiosyncratic jump intensity implies that, in expectation, about 1 idiosyncratic jump happens every 200 years.[26] Idiosyncratic jumps in the model are thus infrequent but their estimated size will essentially make them jumps to default. We further fix the systematic jump intensity parameter, η_m, to 151. Given that the physical jump intensity is defined by η_m times V_t, the values chosen for η_m combined with the average level of V_t subsequently estimated implies that about one systematic jump occurs on average per year. While idiosyncratic jumps are assumed to be rare in the model, systematic jumps on the other hand are assumed to be more frequent although their expected jump size will be estimated to be less consequential for firms' default risk. This leaves us with 12 structural parameters to estimate, $\Theta \equiv \{\Psi_m, \Psi_j\}$ with $\Psi_m \equiv \{\kappa, \theta, \delta, \rho, z_m, \gamma_m, \xi_{A\perp V}, \xi_V, \xi_m\}$ and $\Psi_j \equiv \{\sigma_j, z_j, \gamma_j\}$, and two latent variables, A_t^r and V_t, to filter. To do so, we adopt a daily observation frequency and assume that the 5-year CDX spread ($S_{5,t}^{\text{CDX}}$) and the physical conditional SPX volatility (σ_t^{SPX}) are observed without errors (e.g., Duffee, 2002; Aït-Sahalia and Kimmel, 2010). To proxy σ_t^{SPX}, we use the conditional volatility estimated by fitting a NGARCH-model featuring asymmetric t-distributed innovations on SPX returns. We then filter $\hat{A}_t^r$ and $\hat{V}_t$ from $S_{5,t}^{\text{CDX}}$ and σ_t^{SPX}, on each day t, by solving the following two equations

$$S_{5,t}^{\text{CDX}} = S(\hat{A}_t^r, \hat{V}_t, 5, \Theta) \quad \text{and} \quad \sigma_t^{\text{SPX}} = \sqrt{\sigma_E^2(\hat{A}_t^r, \hat{V}_t, \Theta)}, \tag{16}$$

where we have imposed firm homogeneity $\hat{A}_t^j = \hat{A}_t^r$. In the previous equations, S is defined by equation (11) and σ_E^2 for the SPX index satisfies equation (15) in Proposition (2) when g is an index written on E in equation (10). On the one hand, risk-neutral pricing implies that the level of the CDX term structure embeds relevant information about the economy $\mathbb{Q}$-dynamics. On the

[25] Fixing the jump intensity while estimating the jump distribution is a common practice in the jump literature given the rare nature of idiosyncratic jumps and the challenge in precisely identifying both jump intensity and distribution together.

[26] Note that our assumed idiosyncratic jump intensity is of the same order of magnitude as the one in Collin-Dufresne, Junge, and Trolle (2021).

other hand, taking the conditional volatility of SPX returns to be an "observable" is important because it is informative about model $\mathbb{P}$-dynamics. Furthermore, inherent differences in the payoffs of the claims composing the CDX and SPX indices implies that fitting the CDX level jointly with the SPX physical volatility is thus not only informative about $\mathbb{P}$- and $\mathbb{Q}$-dynamics but also about the decomposition of total asset risk into diffusive and jump risks as both risks impact the pricing of credit instruments and equities differently. Details about the computation of $S(A_t^r, V_t, 5, \Theta)$ and $\sigma_E^2(\hat{A}_t^r, \hat{V}_t, \Theta)$ for a given pair of A_t^r and V_t are provided in Appendix A and Appendix C.2.

Our estimation strategy further postulates that 3-, 7-, and 10-year CDX spreads are observed with Gaussian errors such that

$$S_{T,t}^{\text{CDX}} = S(A_t^r, V_t, T, \Theta) + e_{T,t}, \tag{17}$$

for $T = 3,\ 7,\ 10$, and where $e_{T,t} \sim N(0, \sigma_e^2)$. Based on these assumptions, we estimate Θ via maximum likelihood by solving the following maximization problem

$$\hat{\Theta} \equiv \text{argmax} \log \mathcal{L}(\Theta) = \text{argmax} \sum_{t=2}^{T} \log \mathbb{P}\left(Y_t \mid Y_{t-1}; \Theta\right), \tag{18}$$

where $Y_t = \left\{S_{3,t}^{\text{CDX}}, S_{5,t}^{\text{CDX}}, S_{7,t}^{\text{CDX}}, S_{10,t}^{\text{CDX}}, \sigma_t^{\text{SPX}}\right\}$ is the vector of observables on day t. Note that the distribution of the filtered state variables and the impact of mapping $\{\hat{A}_t^r, \hat{V}_t\}$ to the vector of observables Y_t is taken into account when computing $\mathbb{P}\left(Y_t \mid Y_{t-1}; \Theta\right)$. Details about the construction and computation of the likelihood function in our framework are provided in Appendix C.

4 Model Fit

Our empirical evaluation of our model's goodness-of-fit is composed of three parts. First, we discuss estimated parameters in light of the results documented in the literature. In the second part, we study the model's in-sample fit for the term structure of CDX spreads and SPX return volatility. Finally, we analyze the out-of-sample performance of the model in explaining jointly the pricing

of two derivatives markets: the CDX swaption and SPX option markets. Model implications for option expected returns traded in these two markets are discussed in Section 5.

4.1 Estimation Results

Table 1 presents the 21 structural parameters of our model. Recall that nine parameters are calibrated and are presented in Panel A. The remaining parameters in Panel B are estimated via maximum likelihood following the strategy outlined in the previous section. The first four rows of Panel B reports on the parameters governing systemic asset variance dynamics. The estimated mean reversion speed ($\hat{\kappa}$) is 2.73. This value corresponds to a daily persistence of $1 - 2.73/365 = 0.9925$ which is comparable to the persistence of variance reported for large equity indices (see, e.g., Bates, 2000; Pan, 2002). The long-run mean of systematic variance, $\hat{\theta}$, is 0.67% which translates into a yearly volatility level of $\sqrt{0.67\%} = 8.19\%$. The volatility of variance parameter is 18.79% and the correlation $\hat{\rho}$ between the two systematic Brownian motions $W_t^{A\perp V}$ and W_t^V is -0.62. Apart from the level of asset systematic variance which is lower than for equity index because of the impact of firm financial leverage, the remaining estimates for systematic asset variance are comparable to parameters reported in Bates (2000), Pan (2002), and Christoffersen, Fournier, and Jacobs (2018) for the dynamics of the SPX index variance.

The next two parameters reported in rows 5-6 capture diffusive risk compensation. The estimated market price of asset (specific) diffusive risk ($\hat{\xi}_{A\perp V}$) is equal to 0.20 while the market price of variance risk ($\hat{\xi}_V$) is -7.74. Combined, $\hat{\rho}$, $\hat{\xi}_{A\perp V}$, and $\hat{\xi}_V$ implies that the estimated asset premium attributed to diffusive risk satisfies $\left(\sqrt{1-\hat{\rho}^2}\hat{\xi}_{A\perp V} + \hat{\rho}\hat{\xi}_V\right) \cdot V_t = 4.95 \cdot V_t$ in equation (7). Unconditionally, this translates to $4.95 \cdot \hat{\theta} = 3.29\%$ annually. Moreover, the estimated risk-neutral mean reversion speed and unconditional variance are $\hat{\kappa}^{\mathbb{Q}} = \hat{\kappa} + \hat{\delta}\hat{\xi}_V = 1.28$ and $\hat{\theta}^{\mathbb{Q}} = \hat{\kappa}\hat{\theta}/\hat{\kappa}^{\mathbb{Q}} = 1.42\%$, respectively. The negative $\hat{\xi}_V$ estimated thus translates into a more persistent variance process and a higher unconditional level of variance under $\mathbb{Q}$ than under $\mathbb{P}$. This finding is consistent with a wealth of evidence on the presence of a negative variance risk premium.[27]

[27] See, among many others, Todorov (2010b) or Carr and Wu (2009b).

The parameters reported in rows 7-9 in Panel B govern the systematic jump distribution and the market price of systematic jump risk. The mean ($\hat{z}_m$) and volatility ($\hat{\gamma}_m$) of systematic jumps are -1.66% and 1.84%, respectively. Unconditionally, the systematic $\mathbb{P}$-jump intensity is $\eta_m \cdot \hat{\theta} = 1.0049$. Together, these numbers imply that about one systematic jump happens every year causing an approximate -1.63% (i.e., $e^{\hat{z}_m^2 + \frac{\hat{\gamma}_m^2}{2}} - 1$) return on assets. The systematic jump market price of risk parameter is negative and equals -6.24. This estimate implies that the average systematic jump size is more negative under $\mathbb{Q}$ than under $\mathbb{P}$. We have $\hat{z}_m^{\mathbb{Q}} = \hat{z}_m + \hat{\xi}_m \hat{\gamma}_m^2 = -1.87\%$ (v.s. -1.66%). In terms of contribution to the total asset risk premium ($\mu_t - r$), the unconditional systematic jump component obtained by setting V_t to $\hat{\theta}$ in $\lambda_t^m \mathbb{E}_t\left[\tilde{\nu}_t^m\right] dt - \lambda_t^{m,\mathbb{Q}} \mathbb{E}_t^{\mathbb{Q}}[\tilde{\nu}_t^{m,\mathbb{Q}}]$ is equal to 0.42%. This number amounts to a 11.39% contribution of jumps to the total asset risk premium.

Finally, in rows 10-12 we report estimated idiosyncratic diffusive volatility and jump distribution parameters. The estimated diffusive idiosyncratic volatility is 9%, the mean of idiosyncratic jumps is -99%, and idiosyncratic jump volatility is 47%. Combined, the mean and volatility of idiosyncratic jumps imply that one idiosyncratic jump on average causes a -62.85% (i.e., $e^{\hat{z}_j^2 + \frac{\hat{\gamma}_j^2}{2}} - 1$) return on assets. Although these idiosyncratic events are disastrous for the firm, they are relatively infrequent given the idiosyncratic jump intensity calibrated which implies that such event happen every 200 years on average.

A well-known shortcoming of misspecified structural models, when estimated to fit credit spreads, is to imply excessive asset Sharpe ratios or market leverage to fit the data. To gain further confidence in our estimated parameters, it is thus useful to study the aforementioned measures implied by the model. The unconditional asset premium, sum of diffusive (3.29%) and jump compensation (0.42%), is 3.71% annually and the representative firm asset Sharpe ratio is 26%. These estimates compare well to similar measures discussed in the literature. For instance, Chen, Collin-Dufresne, and Goldstein (2009) discuss the importance and economic magnitude of asset Sharpe ratios in structural models. They calibrate a ratio of 22% to a representative Baa firm which is close to our fitted value. Moreover, the fitted level of asset volatility in structural models is only meaningful when discussed in light of firm's market leverage. For instance, a low leverage

could be compensated by a high level of asset volatility and, reciprocally, an inflated market leverage could translate into an abnormally low level of asset volatility. The market leverage of the representative firm implied by the model is 46.11% which is of the same order of magnitude as empirical estimates of leverage for our sample of firms.[28]

Recall that we filter the state variables from the 5-year CDX spread ($S_{5,t}^{\text{CDX}}$) and SPX index conditional volatility (σ_t^{SPX}) by solving $S_{5,t}^{\text{CDX}} = S(\hat{A}_t^r, \hat{V}_t, 5, \hat{\Theta})$ and $\sigma_t^{\text{SPX}} = \sqrt{\sigma_E^2(\hat{A}_t^r, \hat{V}_t, \hat{\Theta})}$ for $\hat{A}_t^r$ and $\hat{V}_t$. Figure 2 presents the filtered time series of the two state variables back out by the estimation procedure. From the figure we see that the two state variables behave as expected. Asset value displays pro-cyclical patterns while fluctuations in systematic variance are rather counter-cyclical. For instance, note the way the representative firm asset value drops on the onset of the Global Financial Crisis (GFC). Around the same period, systematic asset variance increases abruptly. At the same time, observed 5-year CDX spread was approaching 250bps while SPX volatility was close to 75%. At the far right side of the figure we see that the two state variables behave similarly to the GFC period at the beginning of the Covid crisis, which is to be expected.

We conclude that the model parameters are reasonable and produce total asset risk premium, Sharpe ratio, and market leverage that are economically meaningful. The filtered state variables display pronounced time variations matching well economic conditions and our prior about the behavior of these variables around crisis periods.

4.2 In-Sample Fit

We now examine the in-sample fit of our model. Panels A and B of Table 2 present the mean and standard deviation of the CDX spreads and physical SPX volatility in the data and for model fitted values. Since the model is estimated to exactly match 5-year CDX spread and the physical

[28] On average, the market leverage, calculated as the ratio of total liabilities (Compustat item LTQ) to market equity plus total liabilities, is 41% across firms in the SPX and is 49% across firms that belong to both the SPX and the CDX.

SPX volatility, the main variables of interest are 3-, 7-, and 10-year CDX spreads. Accordingly, Panel C reports the time-series correlation of data and model CDX spreads for these maturities as well as model root mean square errors (RMSE).

From Panel A we see that the empirical term structure of CDX spreads is, on average, upward sloping. The spread rises from 56.25 basis points for for the three year maturity to 108.45 basis points when the maturity increases to ten years. Another interesting stylized fact of the CDX market is that long-term CDX spreads are less volatile than short-term ones. While the standard deviation is 42.66 basis points for the three year spread, the ten year maturity has a volatility of 25.95 basis points.

Our model captures these stylized facts relatively well as can be seen from Panel B. The model implied averages and standard deviations are close to their data counterparts. For instance, the three year CDX spread is 51.16 on average in the model, which is close to the empirical average of 56.25. For the long end of the term structure, the average ten year spread in the model is slightly higher than in the data (128.46 vs. 108.45). In terms of spread standard deviations, we see that the model volatility estimates are of the same order of magnitude as the empirical ones but that the term structure of volatility implied by the model is somewhat flatter in the model than in the data.

To provide further insight into our model's ability to explain CDX spreads, we consider 2 diagnostic metrics: the correlation and RMSE between the data and model series which we report in Panel C. First of all, data and model spreads are highly correlated. The correlation estimates range from 0.87 to 0.96 which is encouraging and indicates that the model is able to capture time-series fluctuations in spreads well. In terms of pricing errors, the RMSE estimates range from 15.07 to 27.23. Considering the structural nature of our approach, these estimates are reasonable and comparable to the pricing errors reported in the literature.[29]

In Figure 3, we plot the data and model time-series of CDX spreads and SPX volatility over

[29]Unlike reduced-form frameworks where price dynamics are exogenously specified to fit the data best, our structural approach is relatively less flexible, as price dynamics are endogenously determined from the firm's asset dynamics.

time. For the 5-year CDX spread in Panel B and physical SPX volatility in Panel E, the data and model series perfectly coincide, except for model volatility at the peak of the 2008 financial crisis when the SPX volatility was close to 75%. Panels A, C, and D illustrate the model's ability to capture time variations in spreads. From the figure we see that most of model pricing errors for spreads reported in Table 2 cluster around the financial crisis, which is to be expected. Outside of this period, the model fit closely the data.

The fact that the model is able to generate reasonable averages and time variation of CDX spreads is only meaningful if the model simultaneously produces reasonable values for other relevant variables such as default probability, asset Sharpe ratio, or leverage. For example, if the model were to generate large CDX spreads while predicting excessively high physical default probabilities, then, the model would fall into the trap of the credit spread puzzle. To build further confidence in the quality of model fit, we compare model implied cumulative physical default probability with Moody's estimates. In-sample, the average 10-year cumulative physical default probability generated by the model is 2.57%, which is close to the historical 10-year default rate for investment grade entities reported in Moody's credit report (2.16% for 1983-2018 and 2.29% for 1998-2018).

Overall, the results presented so far suggest that the model is able to fit in-sample the term structure of CDX spreads and SPX physical volatility well, both in terms of level and time-series fluctuations, while predicting reasonable $\mathbb{P}$-metrics (see Section 4.1). We now turn to a much more stringent test of model performance: the analysis of its goodness of fit for equity and credit index derivative markets out-of-sample.

4.3 Out-of-Sample Fit

We consider two tests to assess out-of-sample model fit. The starting point of our analysis is to study the ability of the model to generate reasonable unconditional levels of implied-volatilities for SPX options across the surface and accurate times-series of ATM implied-volatilities. In a second step, we study model out-of-sample predictions for CDX swaptions along the same dimensions.

4.3.1 SPX Options

The option literature highlights the importance of variance and jump risks to explain index options' implied volatilities. Nevertheless, the ability of standard reduced-form models in explaining SPX option returns remains the subject of debate. Before providing our contribution to this discussion, the first logical step is to demonstrate our model's ability to generating reasonable SPX implied volatilities.

So far, most approaches in the option literature consist in fitting reduced-form option pricing models directly to the data on which they are subsequently evaluated. It is worth emphasizing that our model is estimated using the term structure of CDX spreads and SPX physical volatility, but without any price information from SPX options. It is thus natural to ask whether the model's good performance in fitting equity index physical volatility and CDX spreads spills over to SPX option implied-volatilities out-of-sample. The out-of-sample nature of this exercise contrasts with the standard approach and strong performance here can be seen as a contribution in itself.

In Figure 4, we juxtapose the average Black-Scholes-implied volatilities of SPX options calculated from the data (black bars) and from model option prices (grey bars). A few remarks are in order. Overall, the model implied volatilities match their empirical counterparts well. The economic magnitude of the discrepancy between the data and model implied volatilities is relatively small on average. We see that the model generates a pronounced negative volatility skew as in the data.

To quantify model performance, Table 3 reports the average and standard deviation of implied volatility in the data (Panel A) and for the model (Panel B). We further report the time-series correlation between data and model implied volatilities and model RMSE in Panel C. The magnitude of the pricing errors varies across moneyness and maturity. The model tends to underprice OTM puts, particularly at shorter maturities, contracts that are notoriously hard to fit. In contrast, the model overprices ITM puts on average. Impressively, it provides an almost perfect fit for ATM options with three months to expiration, but slightly underestimates one and six month ATM implied-volatilities. Most importantly, the model generates reasonable time-series fluctuations of

implied-volatilities, and this, through the entire surface. Note that the standard deviations of model-implied volatilities are close to those found in the data. This observation is reinforced by the high correlation between data and model implied volatilities reported in Panel C. Finally, the model RMSE ranges from 4.07% to 5.23%. For comparison, Fournier and Jacobs (2020) report an average RMSE of 3.29% for the Heston (1993) model fitted directly to SPX options although their sample does not include the COVID crisis.

In Figure 5, we plot the time-series of one, three and six month expirations ATM implied-volatilities for the data (in dark) and the model (in grey). The model-implied volatilities closely track the time-series fluctuations in the data. Note that the spikes in implied volatilities predicted by the model during the global financial crisis, the sovereign debt crisis, and at the beginning of the COVID period coincide almost perfectly with the data.

In light of these results, we conclude that the model characterizes the SPX option implied volatility surface both unconditionally and in the time-series relatively well.

4.3.2 CDX Swaptions

Our second out-of-sample exercise consists in testing whether our model can predict prices for CDX index options, or swaptions. CDX swaptions are relatively new financial instruments that began trading with significant volumes in 2012.[30] We focus here on CDX swaptions written on the 5-year CDX. So far, evidence in the literature suggests that jointly pricing CDX swaptions and SPX options is challenging (e.g., see Collin-Dufresne, Junge, and Trolle, 2021).

Similarly to SPX options, we compare, in Figure 6, the average Black-implied volatilities for CDX swaptions calculated from quoted prices (black bars) and from model predicted prices (grey bars). There are no clear disparities, and if anything, the fit of the model is better than that obtained for SPX options. The model generates a positive volatility skew which aligns well with the data. Intuitively, a left tail event in the equity market (low equity return) is associated

[30]For details on the pricing and market conventions about CDX swaptions, we refer to Chen, Doshi, and Seo (2021) and Collin-Dufresne, Junge, and Trolle (2021).

with a right tail event in the credit market (high credit spread). Therefore, a negative volatility skew for SPX options is consistent with a positive volatility skew for CDX swaptions. For CDX swaptions, the model slightly overprices options with shorter expirations of one and six months but underprices the longest maturity ones. Overall, the model implied volatilities match their empirical counterparts well unconditionally.

In Table 4, we investigate the pricing performance in more detail. The implied volatility errors are homogenous across the board and fluctuate around 2% in absolute value. Moreover, the model generates reasonable time-series fluctuations of implied-volatilities. For instance, the standard deviations of model-implied volatilities are similar in magnitude to those estimated from quoted prices. The quality of model fit is also confirmed by the high level of correlation between data and model implied volatilities reported in Panel C. Interestingly, while the model matches the CDX volatility surface better unconditionally than SPX options its time-series fit is somewhat lower as suggested by the lower correlation and higher RMSE estimates obtained. Note that the pricing errors reported in Collin-Dufresne, Junge, and Trolle (2021) when fitting a model similar to ours to SPX options to price CDX swaptions out-of-sample is about 28% in absolute value (v.s. 2% in our case), and their model RMSE around 30% (v.s. 10%).

Our assumptions about the representative firm asset dynamics are essentially the same as Collin-Dufresne, Junge, and Trolle (2021) and the only difference between our respective models lies in the way that a firm's capital structure is set up. In Appendix D, we show that the discrepancies in pricing performance for SPX and CDX derivative markets between our two studies cannot be explained by the difference in the way that capital structure is modeled, but rather by the estimated parameters describing asset dynamics. More precisely, using the parameter estimates for asset dynamics reported in Collin-Dufresne, Junge, and Trolle (2021) applied to our set-up, we replicate their main results.[31]. We find that SPX options are overpriced when using the parameters reported in their study obtained by fitting CDX swaptions. Moreover, CDX

[31]For this exercise, the values used for distress costs (α), corporate tax rate (ζ), recovery rate (R), risk-free interest rate (r), asset payout rate (q), coupon payment (c), and default boundary (A_D) are the same as the ones reported in Panel A of Table 3.

swaptions are underpriced when using the set of parameters they estimate when fitting SPX options. We discuss our results for SPX options and CDX swaptions in light of Collin-Dufresne, Junge, and Trolle (2021) in more detail in Appendix D, and document that our estimated CDX spread distribution is much closer to the empirical distribution in terms of skewness and kurtosis.

To visualize the quality of our model's predictions over time, Figure 7 plots the time-series of one, three and six month CDX swaption at-the-money implied volatilities for the data (in black) and the model (in grey). While the model tracks the time-series patterns for ATM implied volatilities fairly well, we do see a few outliers. These correspond to episodes when the stock market declined and fitted asset volatility spiked. In turn, these abrupt increases in volatilities translated into excessive implied volatilities. Nevertheless, apart from these outliers, the time-series fit of the model for CDX swaptions is generally good - the correlation is about 70%.

Having validated our model's performance in fitting the CDX index in sample and SPX and CDX options out of sample, we now turn to using our model to study option returns.

5 Option returns

Equity index option returns have been studied previously but the issue of whether observed return levels are reasonable or offer evidence of mispricing is still under debate. Much less is known for CDX swaption markets. We revisit this question for equity index options and provide new evidence for credit index options. We do so with a model that can predict option return levels without relying on option data in the estimation. Our model also allows us to attribute ex ante return risk premia to asset risk, variance risk and jump risk. Figure 1 as well as Tables 5 and 6 summarize our main findings relating to options returns. We first consider the equity index option market.

5.1 Equity index options

The predicted instantaneous return for the index is about 10% while the realized is a bit lower at 7.81%. As expected, option returns are much higher in absolute magnitude. Bondarenko (2014)

finds in a sample from 1987-2000 that one month at-the-money equity index puts had an annual return of -468 %. In an overlapping sample from 1987 - 2005, Broadie, Chernov, and Johannes (2009) find average at-the-money one month put returns to be -360%. During our more recent sample, these contracts returned -306%. Our model predicted an instantaneous put return of -229%. The corresponding call contracts earned a 150% return compared to the predicted 161%.

Table 5 reports predicted returns and their data counterparts for varying degrees of moneyness. We also report confidence bounds for these allowing us to state whether average realized returns are statistically significantly different from our model's predictions.

Turning to the question of mispricing, we note that for SPX options, all average returns lie within 90% confidence bounds. Hence, similar to our findings for implied volatility levels, we find no evidence of any systematic bias in terms of returns. This finding echoes BCJ although in the context of a richer model which accounts for risk premia both on stochastic volatility and systematic jumps. They test whether the data deviates from simulated option returns in the Black and Scholes (1973) and Heston (1993) models and find no significant evidence of mispricing. More recently, Chambers, Foy, Liebner, and Lu (2014) revisit their study with a longer sample and find more mixed results for the same two models. Hence our results for SPX options align with the earlier conclusion of no mispricing.

Using Proposition 1, we can decompose the predicted return into components relating to diffusive asset risk, variance risk and jump risk. The decomposition is reported in Table 5. Figure 8 shows the elasticities of the different instruments to the three sources of risk embedded in our model. We see from this Figure that puts and calls have opposite sign elasticies with respect to diffusive asset risk and jump risk, while for variance risk they have the same sign.

For the equity index, the main driver of returns is the diffusive unlevered asset risk component (see the last three rows in Table 5 and panel A in Figure 8). Jumps explain about a tenth, while the contribution of variance risk is negative although negligible (panels B & C). The negativity derives from the elasticity of equity, as a call on the firm's assets, being positive. This offsets the effect of variance risk on unlevered asset returns for equity by requiring a lower risk premium. As

we discuss below, the opposite is true for credit.

Like for the index returns, our model allows us to attribute predicted option returns to different sources of risk. Take at-the money equity index puts for example. Consistent with the index itself, diffusive unlevered asset risk is the main driver (72% of the total return), followed by variance risk (17%) and jump risk (11%). However, it is interesting to note that while the index itself draws virtually no return compensation from variance risk, it does matter significantly for the options, in particular out-of-the money contracts. In Figure 8 we see that the latter have higher elasticities in absolute terms. This greater importance for variance risk in the derivative than the underlying asset is noteworthy given that it has been argued that variance risk is unlikely to matter for an option given the short time during which stochastic variance and associated risk premium can influence the underlying dynamics of the underlying.[32]

5.2 Credit index options

Table 6 reports our findings for credit options. The predicted annualized instantaneous credit index return is 1.90 %, whereas the realized return is xxxx %. Consider next at-the-money CDX calls (or payer swaptions) which are economically most similar to puts calls. Their realized returns were -491% compared to our model predicted -327%. The difference is not statistically significant. It is also interesting to note that although these contracts are similar to SPX puts (they pay out in adverse states of the world), their returns are much higher. The predicted (data) returns are 43% (61%) higher. For out-of-the money calls, realized average returns do fall outside a 90% confidence interval, although not a 95% interval. Out-of-the money puts offer the only significant suggestion of any mispricing. For at-the-money and in-the money calls and puts all returns lie within 95% bounds.

Although the predicted and realized returns do differ in economic magnitude for one particular contract, Figure 1 illustrates that broadly speaking, our model's predictions and data realizations line up strikingly well. In addition, when the predicted return for a contract differs from the

[32]See for example Broadie, Chernov, and Johannes (2009).

realized average return, it is still able to identify the relationship in returns between SPX and CDX contracts. For example, the ratio between the model predicted at-the-money CDX call and SPX put returns is 1.43 whereas in the data, the ratio is 1.61.

Turning to the attribution of returns to the three risk sources in our model consider first the index itself. In contrast to the equity index, which resembles a call option on the underlying assets, selling credit insurance using the CDX index implies a short put on the firms' assets (see Merton (1974)). Selling credit insurance is analogous to holding firms' bonds is rewarded with positive ex ante returns.

The largest component for the credit index, explaining about two thirds of the return is diffusive asset risk. Variance risk explains about a quarter, and jump risk eight percent. The higher exposure to variance risk can be explained as follows: holding the unlevered assets requires a positive risk premium to compensate for variance risk, holding firms' credit requires additional compensation for variance risk arising from the "short put". This can be seen from the large negative elasticity in panel B of Figure 8, keeping in mind that the variance risk premium is negative. This is the opposite effect to the case of the equity index, where the long call embedded in the equity has a positive and much smaller elasticity, offsetting some of the positive risk premium inherent in the unlevered assets.

This greater exposure to variance risk is inherited by credit index options. For at-the-money CDX calls, variance risk is the dominant driver of returns (at 56% to 59% depending on moneyness) whereas for puts the impact is somewhat smaller (31 to 39%). Jumps matter less at around 6%, compared to 10% for SPX options.

An interesting result emerges for CDX options. In contrast to the equity index case, calls and puts have opposite elasticities with respect to variance risk. CDX calls with an inherent short credit exposure derive a negative ex ante return from their unlevered asset exposure, similar to SPX puts. Like the equity puts, CDX calls have a positive variance risk elasticity and thus earn more negative returns as a result. However, while SPX calls have a positive variance risk elasticity, CDX puts do not. So while these contracts innately benefit from volatility as options, the long

credit exposure from the underlying index with its large negative elasticity offsets this and makes CDX puts require a larger ex ante return as a result. This explains the asymmetry between the elasticities in panel H of Figure 8 for CDX options in contrast to the near perfect similarity for SPX puts and calls in panel E.

Another interesting regularity is that the importance of variance risk is higher the further away from the money equity index options are, while for CDX options this effect is much weaker.

In summary, our model predicts returns that are consistent with what we observe in the data for all SPX options and most CDX contracts. When we decompose the model-implied returns we find that although both types of options share the same underlying state variables, their loadings on different risks and degrees of embedded leverage make CDX and SPX options quite different contracts. CDX options tend to be larger in absolute terms and behave differently with respect to variance risk than their SPX counterparts.

6 Conclusion

In this paper, we build an internally consistent model for the valuation of corporate securities, credit derivatives, and more specifically (compound) options on both credit and equity indices. We find that such a model, consistent with the pricing of credit spreads and historical equity volatility levels, is able to predict levels of implied volatility for equity and credit options well out-of-sample. It does slightly better in the time series for equity options than for credit spread options.

After validating our model by gauging its out-of-sample performance for levels of option prices, we consider realized and model-predicted option returns. The model does remarkably well at explaining average returns for the underlyings and options on both equity and credit indices. We do not find any evidence of mispricing across the two asset classes - although options returns are strikingly high on average, our model finds these to consistently compensate for the embedded amount of leverage and risk in the underlying indices.

Our models allows us to attribute components of returns to diffusive asset returns, a variance

risk premium and a premium for systematic jumps. We find that equity and credit options are quite different than their equity counterparts. Not only do they appear to be more leveraged and earn larger absolute returns on average, their risk attribution differs as well. Credit option returns depend more on a variance risk premium than their equity equivalents. This observation holds true also at the index level, where credit index returns compensate significantly for variance, while equity index returns barely do. Jumps matter more for equity options.

In terms of direct extensions of our framework, there are two avenues we believe could be fruitful. One is to consider a multifactor setup for the asset variance (see Christoffersen, Heston, and Jacobs, 2009). Another is extending the asset jump setup – it is quite possible that jumps with time-varying default intensities (see, e.g., Duffee, 1999) would help the model do better in jointly explaining the time series of SPX and CDX implied volatilities.

Another area where our model could be applied is in the literature on corporate bond returns. Most work to date on corporate bond returns has been done in model-free regression settings. A model such as the one proposed in this paper could be useful in predicting and explaining expected returns by allowing information to be extracted from several markets simultaneously.

References

Aït-Sahalia, Yacine, and Robert L Kimmel, 2010, Estimating affine multifactor term structure models using closed-form likelihood expansions, *Journal of Financial Economics* 98, 113–144.

Andersen, Torben G, Nicola Fusari, and Viktor Todorov, 2020, The pricing of tail risk and the equity premium: Evidence from international option markets, *Journal of Business & Economic Statistics* 38, 662–678.

Andersen, Torben G, Viktor Todorov, and Masato Ubukata, 2020, Tail risk and return predictability for the Japanese equity market, *Journal of Econometrics, Forthcoming*.

Bates, David S., 2000, Post-'87 crash fears in the S&P 500 futures option market, *Journal of Econometrics* 94, 181–238.

Berger, David, Ian Dew-Becker, and Stefano Giglio, 2020, Uncertainty shocks as second-moment news shocks, *The Review of Economic Studies* 87, 40–76.

Black, Fischer, and Myron Scholes, 1973, The Pricing of Options and Corporate Liabilities, *Journal of Political Economy* 81, 637–654.

Bondarenko, Oleg, 2014, Why are put options so expensive?, *Quarterly Journal of Finance* 4, 1–50.

Broadie, Mark, Mikhail Chernov, and Michael Johannes, 2009, Understanding Index Option Returns, *The Review of Financial Studies* 22, 4493–4529.

Cao, Jie, Amit Goyal, Xiao Xiao, and Xintong Zhan, 2022, Implied Volatility Changes and Corporate Bond Returns, *Management Science* pp. 1–23.

Carr, Peter, and Liuren Wu, 2009a, Variance risk premiums, *Review of Financial Studies* 22, 1311–1341.

Carr, Peter, and Liuren Wu, 2009b, Variance risk premiums, *The Review of Financial Studies* 22, 1311–1341.

Carr, Peter, and Liuren Wu, 2011, A Simple Robust Link Between American Puts and Credit Protection, *The Review of Financial Studies* 24, 473–505.

Chambers, Donald R., Matthew Foy, Jeffrey Liebner, and Qin Lu, 2014, Index Option Returns: Still Puzzling, *The Review of Financial Studies* 27, 1915–1928.

Chen, Long, Pierre Collin-Dufresne, and Robert S Goldstein, 2009, On the relation between the credit spread puzzle and the equity premium puzzle, *The Review of Financial Studies* 22, 3367–3409.

Chen, Steven Shu-Hsiu, Hitesh Doshi, and Sang Byung Seo, 2021, Ex Ante Risk in the Corporate Bond Market: Evidence from Synthetic Options, *Available at SSRN 3345455*.

Cheng, Ing-Haw, 2018, The VIX Premium, *The Review of Financial Studies* 32, 180–227.

Christoffersen, Peter, Mathieu Fournier, and Kris Jacobs, 2018, The Factor Structure in Equity Options, *The Review of Financial Studies* 31, 595–637.

Christoffersen, Peter, Steven Heston, and Kris Jacobs, 2009, The Shape and Term Structure of the Index Option Smirk: Why Multifactor Stochastic Volatility Models Work So Well, *Management Science* 55, 1914–1932.

Collin-Dufresne, Pierre, Robert S. Goldstein, and Fan Yang, 2012, On the relative pricing of long-maturity index options and collateralized debt obligations, *Journal of Finance* 67, 1983–2014.

Collin Dufresne, Pierre, Robert S. Goldstein, and Fan Yang, 2012, On the Relative Pricing of LongMaturity Index Options and Collateralized Debt Obligations, *The Journal of Financ* 67, 1983–2014.

Collin-Dufresne, Pierre, Benjamin Junge, and Anders B Trolle, 2021, How Integrated Are Credit and Equity Markets? Evidence From Index Options, Working Paper.

Coval, Joshua D., and Tyler Shumway, 2001, Expected option returns, *Journal of Finance* 56, 983–1009.

Cremers, K. J. Martijn, Joost Driessen, and Pascal Maenhout, 2008, Explaining the level of credit spreads: Option-implied jump risk premia in a firm value model, *Review of Financial Studies* 21, 2209–2242.

Culp, Christopher L., Yoshio Nozawa, and Pietro Veronesi, 2018, Option-based credit spreads, *American Economic Review* 108, 454–88.

Davydenko, Sergei, 2012, When do firms default? A study of the default boundary, Working Paper, University of Toronto.

Du, Du, Redouane Elkamhi, and Jan Ericsson, 2019, Time-Varying Asset Volatility and the Credit Spread Puzzle, *Journal of Finance* 74, 1841–1885.

Duffee, Gregory R, 1999, Estimating the price of default risk, *Review of Financial Studies* 12, 197–226.

Duffee, Gregory R., 2002, Term premia and interest rate forecasts in affine models, *Journal of Finance* 57, 369–443.

Eraker, Bjørn, Michael Johannes, and Nicholas Polson, 2003, The impact of jumps in volatility and returns, *Journal of Finance* 58, 1269–1300.

Eraker, Bjorn, and Yue Wu, 2017, Explaining the negative returns to VIX futures and ETNs: An equilibrium approach, *Journal of Financial Economics* 125, 72–98.

Feldhütter, Peter, and Stephen M Schaefer, 2018, The myth of the credit spread puzzle, *The Review of Financial Studies* 31, 2897–2942.

Heston, Steven L., 1993, A Closed-Form Solution for Options with Stochastic Volatility with Applications to Bond and Currency Options, *Review of Financial Studies* 6, 327–343.

Israelov, Roni, and Bryan T. Kelly, 2017, Forecasting the Distribution of Option Returns, *Yale School of Management Working Paper*.

Leland, Hayne E, 1994, Corporate debt value, bond covenants, and optimal capital structure, *Journal of Finance* 49, 1213–1252.

Merton, Robert C., 1974, On the pricing of corporate debt: The risk structure of interest rates, *Journal of Finance* 29, 449–470.

Pan, Jun, 2002, The jump-risk premia implicit in options: Evidence from an integrated time-series study, *Journal of Financial Economics* 63, 3–50.

Seo, Sang Byung, and Jessica A. Wachter, 2018, Do rare events explain CDX tranche spreads?, *Journal of Finance* 73, 2343–2383.

Todorov, Viktor, 2010a, Variance risk-premium dynamics: The role of jumps, *Review of Financial Studies* 23, 345–383.

Todorov, Viktor, 2010b, Variance risk-premium dynamics: The role of jumps, *The Review of Financial Studies* 23, 345–383.

Vasicek, Oldrich, 2002, The distribution of loan portfolio value, *Risk* 15, 160–162.

Figure 2: Filtered State Variables

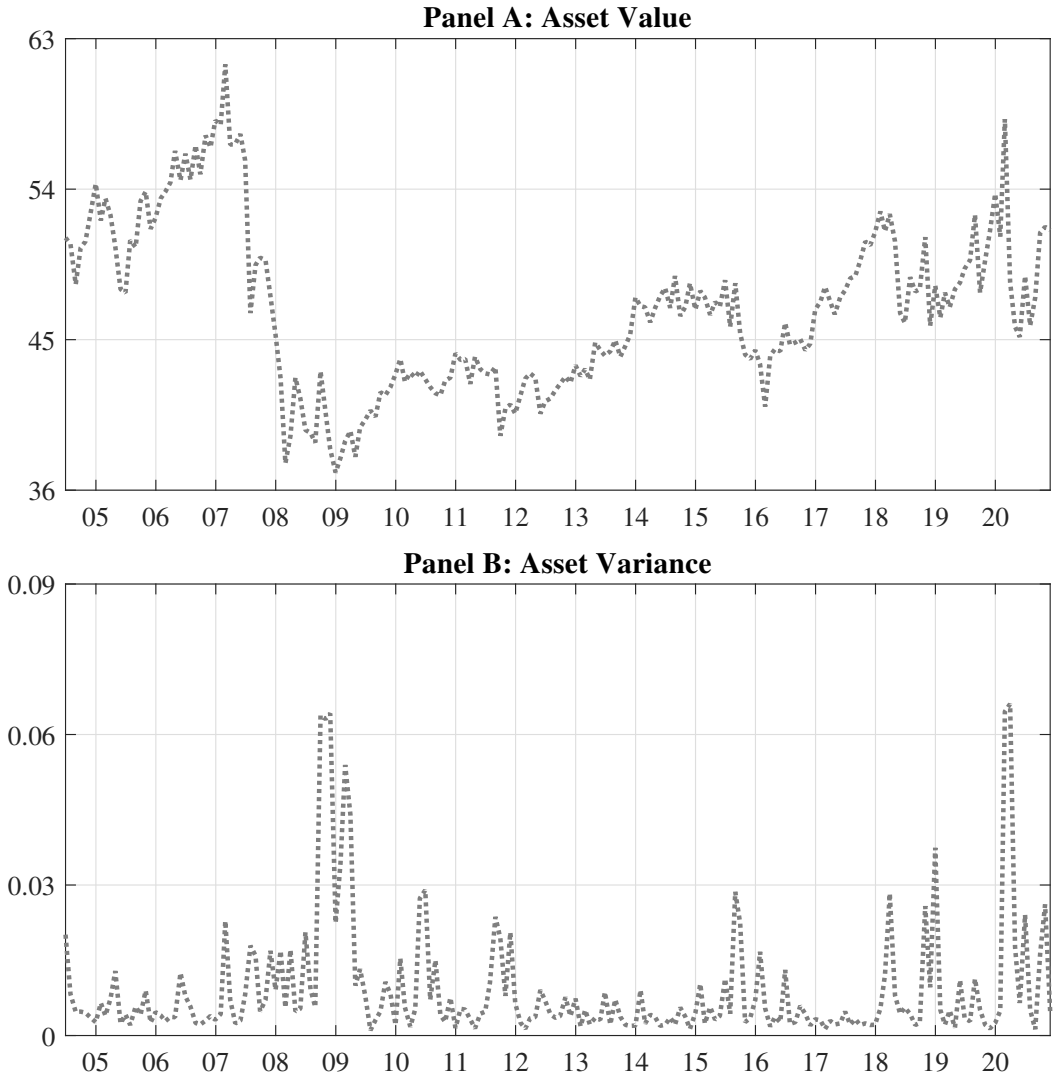

Notes: This figure presents the time series of the two filtered state variables of our model. Panel A plots the filtered asset value A_t^r. Panel B presents the filtered systematic asset variance V_t. The sample period is from June 2004 to November 2020.

Figure 3: Fittted Credit Spreads and Equity Volatility

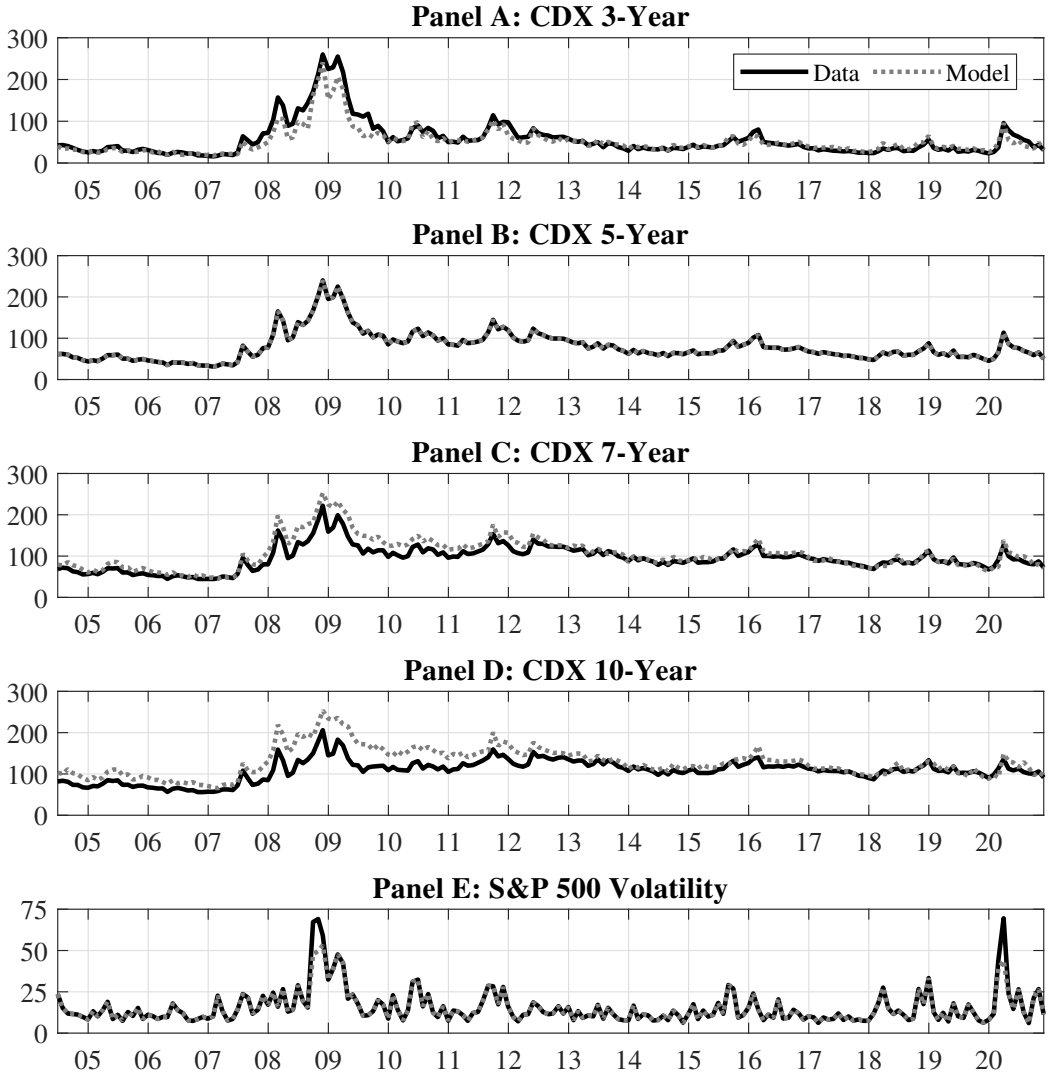

Notes: This figure plots the time series of the five observables in our estimation procedure: (i) 3-year CDX spread, (ii) 5-year CDX spread, (iii) 7-year CDX spread, (iv) 10-year CDX spread, and (v) physical SPX volatility implied by the NGARCH model. The solid lines represent the data, and the dotted lines represent the model. The sample period is from June 2004 to December 2020.

Figure 4: Average Equity Index Volatility Surface: Data vs Model

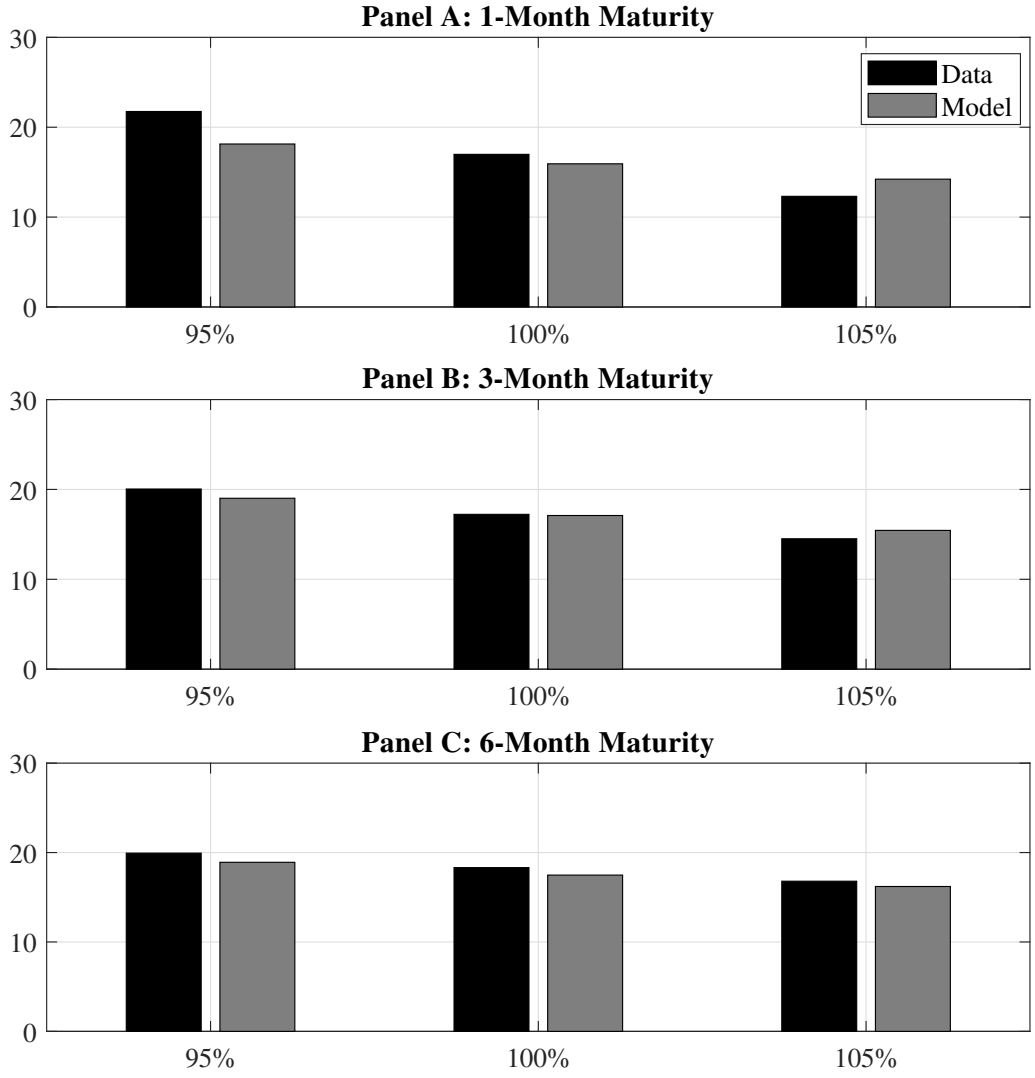

Notes: This figure compares the average Black-Scholes-implied volatilities of SPX options calculated from the data (black bars) and the model (gray bars). We consider three option maturities (1, 3, and 6 months) and three moneyness values (95, 100, and 105%). The sample period is from June 2004 to November 2020.

Figure 5: Time Series of ATM Equity Index Volatilities

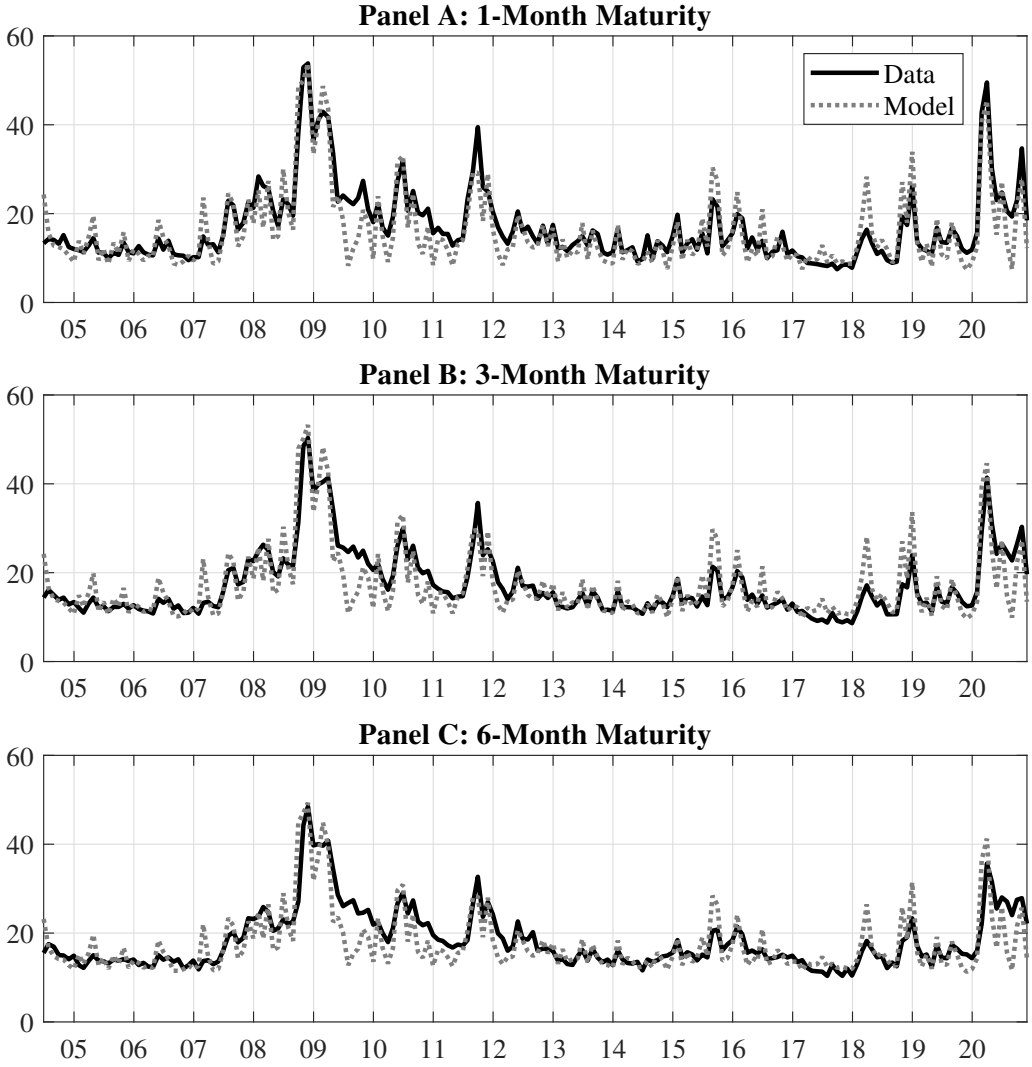

Notes: This figure plots the time series of the SPX ATM implied volatilities from the data and the model. Panels A, B, and C show the results for the 1-, 3-, and 6-month option maturities. The solid lines represent the data, and the dotted lines represent the data. The sample period is from June 2004 to November 2020.

Figure 6: Average CDX Index Volatility Surface: Data vs Model

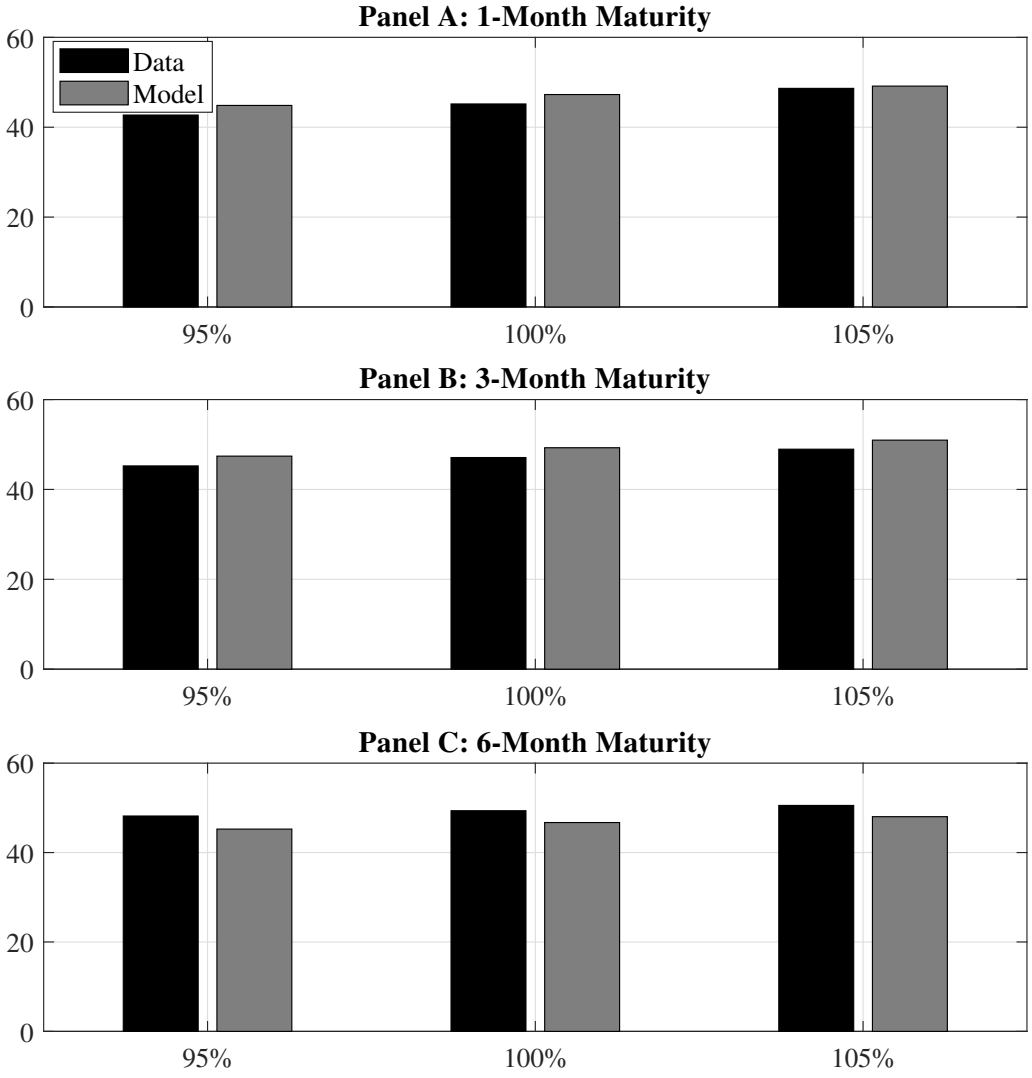

Notes: This figure compares the average Black-implied volatilities of CDX swaptions calculated from the data (black bars) and the model (gray bars). We consider three option maturities (1, 3, and 6 months) and three moneyness values (95, 100, and 105%). The sample period is from March 2012 to November 2020.

Figure 7: Time Series of ATM Credit Index Volatilities

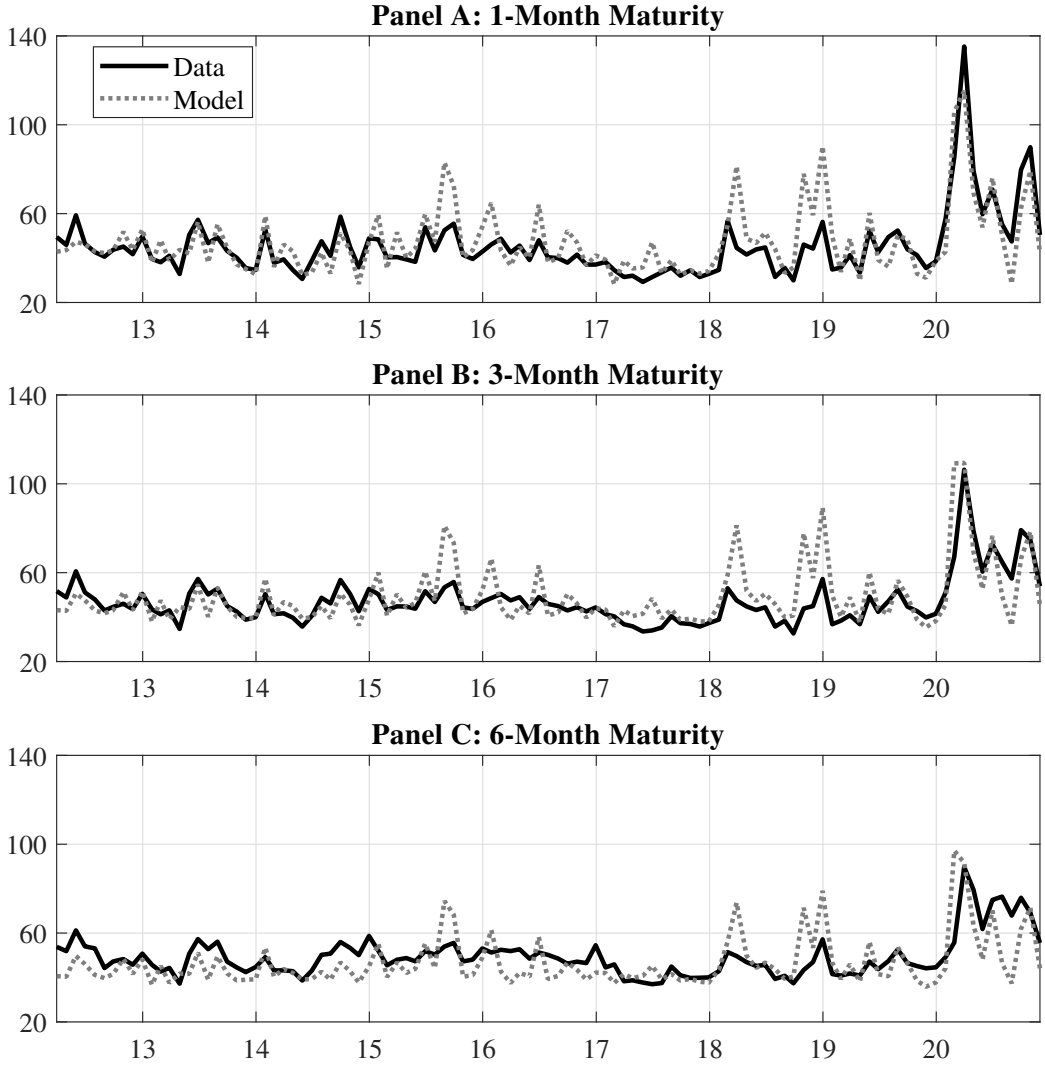

Notes: This figure plots the time series of the CDX ATM implied volatilities from the data and the model. Panels A, B, and C show the results for the 1-, 3-, 6-month option maturities. The solid lines represent the data, and the dotted lines represent the model. The sample period is from March 2012 to November 2020.

Figure 8: Elasticities

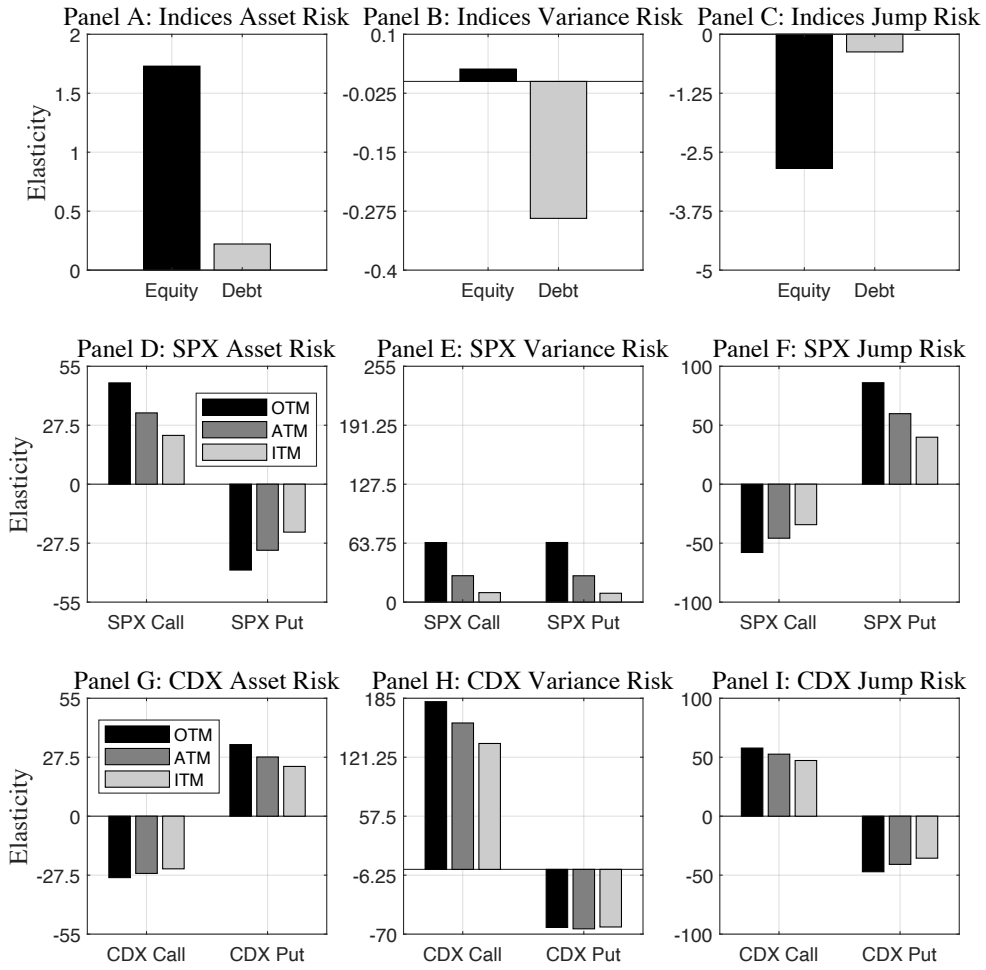

Notes: This figure plots ...

Table 1: Model Parameters

Panel A: Calibrated Parameters	
1-Distress costs (α)	25.00%
2-Corporate tax rate (ζ)	20.00%
3-Recovery rate (R)	51.00%
4-Risk-free interest rate (r)	1.00%
5-Asset payout rate (q)	2.00%
6-Coupon payment (c)	0.25
7-Default boundary (A_D)	19.50
8-Systematic jump intensity loading (η_m: $\lambda_t^m = \eta_m V_t$)	151
9-Idiosyncratic jump intensity (λ^j)	0.50%
Panel B: Estimated Parameters	
1-Mean reversion speed ($\hat{\kappa}$)	2.7289
2-Long run mean ($\hat{\theta}$)	0.67%
3-Volatility parameter for asset variance ($\hat{\delta}$)	18.79%
4-Correlation between asset value and variance shocks ($\hat{\rho}$)	-0.6195
5-Market price of asset specific risk ($\hat{\xi}_{A\perp V}$)	0.2024
6-Market price of variance risk ($\hat{\xi}_V$)	-7.7340
7-Systematic jump size mean ($\hat{z}_m$)	-1.66%
8-Systematic jump size standard deviation ($\hat{\gamma}_m \times 100$)	1.84%
9-Market price of systematic jump ($\hat{\xi}_m$)	-6.2389
10-Idiosyncratic volatility ($\hat{\sigma}_j$)	9.20%
11-Idiosyncratic jump size mean ($\hat{z}_j$)	-99.02%
12-Idiosyncratic jump size standard deviation ($\hat{\gamma}_j$)	0.4692%

Notes: This table reports the values of our model parameters. Panel A presents the parameters that are calibrated. Panel B presents the parameters that are estimated via maximum likelihood estimation.

Table 2: In-Sample Model Fit

	Panel A: Data		Panel B: Model		Panel C: Fit	
	Mean	Std.	Mean	Std.	Corr.	RMSE
CDX 3-Year	56.25	42.66	51.16	32.76	0.96	15.07
CDX 5-Year	79.85	35.77	79.84	35.80	–	–
CDX 7-Year	94.93	29.62	105.46	38.32	0.96	16.60
CDX 10-Year	108.45	25.95	128.46	35.95	0.87	27.23
S&P 500 Vol	15.46	10.40	15.08	8.74	–	–

Notes: This table reports the in-sample fit of our model. There are five observables in our estimation procedure: (i) 3-year CDX spread, (ii) 5-year CDX spread, (iii) 7-year CDX spread, (iv) 10-year CDX spread, and (v) physical SPX volatility implied by the NGARCH model. Panel A reports the mean, standard deviation, and first-order autocorrelation of each variable in the data. Panel B reports the same summary statistics of each variable estimated from the model. Panel C reports three diagnostic measures concerning model fit: the correlation between the data and model series, root mean squared error (RMSE), and mean absolute percentage error (MAPE). The sample period is from June 2004 to November 2020.

Table 3: Out-of-Sample Model Fit: Equity Index Options

	Panel A: Data		Panel B: Model		Panel C: Fit	
K	Mean	Std.	Mean	Std.	Corr.	RMSE
			1-Month Maturity			
95%	21.75	8.04	18.13	8.27	0.89	5.23
100%	16.98	8.32	15.93	8.71	0.89	4.08
105%	12.31	8.70	14.22	8.90	0.89	4.49
			3-Month Maturity			
95%	20.05	7.08	19.02	7.81	0.86	4.07
100%	17.23	7.34	17.10	8.05	0.86	4.08
105%	14.51	7.68	15.44	8.23	0.86	4.37
			6-Month Maturity			
95%	19.93	6.36	18.91	6.84	0.82	4.10
100%	18.31	6.60	17.48	6.94	0.82	4.14
105%	16.80	6.93	16.20	7.01	0.82	4.26

Notes: This table reports the out-of-sample fit of our model for SPX options. Panel A reports the mean, standard deviation, and first-order autocorrelation of each option with a fixed maturity and moneyness. Panel B reports the same summary statistics of each option estimated from the model. Panel C reports three diagnostic measures concerning model fit: the correlation between the data and model series, root mean squared error (RMSE), and mean absolute percentage error (MAPE). The sample period is from June 2004 to November 2020.

Table 4: Out-of-Sample Model Fit: Credit Index Options

	Panel A: Data		Panel B: Model		Panel C: Fit	
K	Mean	Std.	Mean	Std.	Corr.	RMSE
			1-Month Maturity			
95%	42.71	14.18	44.85	16.09	0.76	10.79
100%	45.18	14.24	47.27	15.44	0.77	10.21
105%	48.65	13.97	49.15	14.84	0.78	9.60
			3-Month Maturity			
95%	45.23	10.74	47.41	14.11	0.70	10.29
100%	47.10	10.74	49.28	13.88	0.71	10.06
105%	48.96	10.70	50.97	13.71	0.71	9.84
			6-Month Maturity			
95%	48.18	9.28	45.25	11.44	0.56	10.30
100%	49.35	9.24	46.71	11.40	0.56	10.15
105%	50.54	9.16	48.02	11.37	0.57	10.04

Notes: This table reports the out-of-sample fit of our model for CDX swaptions. Panel A reports the mean, standard deviation, and first-order autocorrelation of each option with a fixed maturity and moneyness. Panel B reports the same summary statistics of each option estimated from the model. Panel C reports three diagnostic measures concerning model fit: the correlation between the data and model series, root mean squared error (RMSE), and mean absolute percentage error (MAPE). The sample period is from March 2012 to November 2020.

Table 5: Model-predicted vs. Data Option Returns: Equity Index

	Index	Call			Put		
		OTM	ATM	ITM	OTM	ATM	ITM
$\mathbb{E}_t\left[\frac{dg_t}{g_t}\right] - E_t^{\mathbb{Q}}\left[\frac{dg_t}{g_t}\right]$ model	10.29%	176.24%	149.78%	117.57%	-342.48%	-229.02%	-148.48%
$\mathbb{E}_t\left[\frac{dg_t}{g_t}\right] - E_t^{\mathbb{Q}}\left[\frac{dg_t}{g_t}\right]$ data	7.81%	148.80%	160.79%	80.77%	-526.06%	-305.84%	-120.29%
Asst risk premium	8.99%	243.29%	171.38%	117.62%	-203.78%	-158.36%	-115.63%
Vol. risk premium	0.27%	-84.10%	-36.15%	-11.66%	-103.46%	-47.32%	-17.91%
Jump risk premium	1.03%	17.05%	14.56%	11.61%	-35.24%	-23.35%	-14.94%
Proportion asset risk premium	87.40%	138.05%	114.42%	100.04%	59.50%	69.15%	77.88%
Proportion vol. risk premium	2.59%	-47.72%	-24.14%	-9.91%	30.21%	20.66%	12.06%
Proportion jump risk premium	10.00%	9.67%	9.72%	9.87%	10.29%	10.19%	10.06%

Notes: This table reports the comparison of the model-implied excess returns for S&P 500 index and its options with the corresponding empirical measures. In the case of index options, the table reports on the comparisons of the model and data returns for out-the-money (OTM), at-the-money (ATM), and in-the-money (ITM) put and call options. We use the parameters reported in Table 1 to compute the model-implied S&P 500 index and its option returns. The empirical counterparts for the index and its options are based on the average monthly returns during our sample. The sample period is from June 2004 to November 2020. The table further provides the decomposition of the model-implied returns into various sources of risk. The last three rows show the proportion of return attributed to each source of risk in our model.

Table 6: Model-predicted vs. Data Option Returns: Credit Index

	Index	Call			Put		
		OTM	ATM	ITM	OTM	ATM	ITM
$\mathbb{E}_t\left[\frac{dg_t}{g_t}\right] - E_t^{\mathbb{Q}}\left[\frac{dg_t}{g_t}\right]$ model	1.90%	-361.87%	-326.78%	-292.25%	259.92%	232.22%	207.59%
$\mathbb{E}_t\left[\frac{dg_t}{g_t}\right] - E_t^{\mathbb{Q}}\left[\frac{dg_t}{g_t}\right]$ data	1.86%	-619.52%	-491.00%	-362.55%	481.36%	303.63%	236.75%
Asst risk premium	1.29%	-137.40%	-125.98%	-114.30%	122.55%	106.72%	93.55%
Vol. risk premium	0.46%	-203.42%	-182.16%	-161.60%	125.55%	114.72%	104.21%
Jump risk premium	0.15%	-21.05%	-18.64%	-16.34%	11.82%	10.78%	9.83%
Proportion asset risk premium	67.86%	37.97%	38.55%	39.11%	47.15%	45.96%	45.07%
Proportion vol. risk premium	24.21%	56.21%	55.75%	55.30%	48.30%	49.40%	50.20%
Proportion jump risk premium	7.93%	5.82%	5.70%	5.59%	4.55%	4.64%	4.74%

Notes: This table reports the comparison of the model-implied excess returns for CDX 500 index and its options with the corresponding empirical measures. In the case of index options, the table reports on the comparisons of the model and data returns for out-the-money (OTM), at-the-money (ATM), and in-the-money (ITM) put and call options. We use the parameters reported in Table 1 to compute the model-implied CDX index and its option returns. The empirical counterparts for the index and its options are based on the average monthly returns during our sample. The sample period for the option returns is from March 2012 to November 2020. The sample period for the credit index is from June 2004 to November 2020. The table further provides the decomposition of the model-implied returns into various sources of risk. The last three rows show the proportion of return attributed to each source of risk in our model.

Appendix

This Appendix contains various theoretical and empirical details complementing the analysis in the core of the paper.

A Pricing details of Firm Credit Derivatives

A.1 CDS risky PV01 and protection leg

A CDS contract involves two parties: the protection buyer and the protection seller. The protection buyer makes quarterly premium payments to the protection seller until the maturity of the contract or until the firm's default. When the running spread paid by the buyer is one basis point (bp) per annum, the present value of future premiums (or premium leg) is called the risky PV01 and is computed in our model as:

$$\text{RPV01}(A_t^j, V_t, T) = 0.0001 \times \sum_{i=1}^{4T} e^{-r(t_i - t)} \left[1 - G(A_t^j, V_t, t_i)\right] / 4,$$

where T is the maturity of the given CDS contract and $\{t_1, t_2, \cdots t_{4T}\}$ denote quarterly premium payment dates, and $G(A_t^j, V_t, t_i) = \mathbb{E}_t^{\mathbb{Q}}\left[\mathbb{1}_{\tau_j \leqslant t_i}\right]$. The present value of a contingent protection payment (or protection leg) is computed as:

$$\text{ProtLeg}(A_t^j, V_t, T) = (1 - R) \sum_{i=1}^{4T} e^{-r(t_i - t)} \left[G(A_t^j, V_t, t_i) - G(A_t^j, V_t, t_{i-1})\right].$$

Here, R represents the recovery rate, which is measured as a fraction of the CDS notional value and is assumed identical across firms for parsimony.

A.2 CDX options

The CDX index is defined as the average basis points default swap spread across the constituent firms,

$$I_t(A_t^1, \ldots, A_t^N, V_t) = \frac{1}{N} \sum_{j=1}^{N} S^j(A_t^j, V_t). \tag{A.1}$$

However, in practice, the index for an investment-grade entity is traded in terms of an upfront fee and a standardized coupon, currently 100 basis points. This fee is the required side payment between the buyer and seller of default insurance to compensate for the difference between the fair market spread and the standardized coupon. The upfront fee is exchanged between the protection buyer and protection seller at the beginning of the contract. For a generic entity, the upfront fee U is determined so that the contract is fair to both parties, namely $U + 100 \times \text{RPV01} = \text{ProtLeg}$. Therefore, the upfront fee for firm j is determined as

$$U(A_t^j, V_t, T) = \text{ProtLeg}(A_t^j, V_t, T) - 100 \times \text{RPV01}(A_t^j, V_t, T). \tag{A.2}$$

While the upfront fee and the CDS spread are two different trading/quoting conventions , they are in fact equivalent. Combining equations (A.2) and (11) results in a simple relation: $U(A_t^j, V_t, T) = \big[S(A_t^j, V_t, T) - 100\big] \times \text{RPV01}(A_t^j, V_t, T)$.

In addition, CDX options provide front-end protection, meaning that if there is a credit event prior to the option expiration, the contract remains active and the holder of a call (payer swaption) obtains the default payment on the CDS. Chen, Doshi, and Seo (2021) show that with front-end protection, credit index swaptions can be viewed as call and put options written on, $\tilde{U}$, an adjusted up-front fee, so that

$$I_t(A_t^1, \ldots, A_t^N, V_t) = \frac{1}{N} \sum_{j=1}^{N} \tilde{U}^j(A_t^j, V_t), \tag{A.3}$$

where $\tilde{U}^j$ is given by

$$\widetilde{U}_t^j = \mathbb{1}_{\{\tau^j > t\}} U_t^j + \mathbb{1}_{\{\tau^j \leqslant t\}}(1-R), \tag{A.4}$$

where $\widetilde{U}_t^j \equiv U(A_t^j, V_t, T)$ is firm j's upfront fee and R is the CDS/bond-specific recovery rate which we assume to be the same across firms. Please refer to Section 3 of Chen, Doshi, and Seo (2021) for further details and examples.

B Firm and Index Contingent Claim Dynamics

In this section, we derive the dynamics of a contingent claim written on a firm's asset dynamics in (2). We will use the results derive here in the next section where we consider the dynamics of a generic index and derivatives on such index constituted of firm contingent claims (i.e., stocks, CDS, etc...).

B.1 Dynamics of corporate contingent claims

To begin, consider a corporate claim or derivative f whose value is determined by the dynamics of the state variables, $f_t^j \equiv f(A_t^j, V_t)$. Using Itô's lemma, we find its return dynamics under $\mathbb{P}$ to be

$$\begin{aligned} df_t^j &= \frac{\partial f_t^j}{\partial A_t^j} dA_{c,t}^j + \frac{1}{2}\frac{\partial^2 f_t^j}{\left(\partial A_t^j\right)^2}\left(dA_{c,t}^j\right)^2 + \frac{\partial f_t^j}{\partial V_t} dV_t + \frac{1}{2}\frac{\partial^2 f_t^j}{\left(\partial V_t\right)^2}\left(dV_t\right)^2 \\ &+ \frac{\partial^2 f_t^j}{\partial A_t^j \partial V_t} dA_{c,t}^j dV_t + dJ_t^{j,f} + dJ_t^{m,f}, \end{aligned}$$

where we use $dA_{c,t}^j$ to denote the continuous dynamics of A_t^j between jumps:

$$dA_{c,t}^j = \left(\mu_t - q\right) A_t^j dt + \sqrt{V_t} A_t^j dW_t^A - \lambda_t^j \bar{\nu}^j A_t^j dt - \lambda_t^m \bar{\nu}^m A_t^j dt + \sigma_j A_t^j dW_t^j,$$

and where we have written the jump dynamics in their shorthand

$$dJ_t^{j,f} = \left(f(A_t^j e^{\tilde{Z}_t^j}, V_t) - f_t^j\right) dN_t^j$$
$$dJ_t^{m,f} = \left(f(A_t^j e^{\tilde{Z}_t^m}, V_t) - f_t^j\right) dN_t^m.$$

Note that the second superscript f in J denotes a jump in the value of f caused by a jump in asset value A_t^j, while the first superscripts j/m identify idiosyncratic/systematic jumps.

Expanding and rearranging, we can write

$$\begin{aligned} df_t^j &= \mu_{f,t}^j f_t^j dt + \frac{\partial f_t^j}{\partial A_t^j} A_t^j \sigma_j dW_t^j + \frac{\partial f_t^j}{\partial A_t^j} A_t^j \sqrt{V_t} dW_t^A + \frac{\partial f_t^j}{\partial V_t} \delta \sqrt{V_t} dW_t^V \\ &+ dJ_t^{j,f} + dJ_t^{m,f} - \frac{\partial f_t^j}{\partial A_t^j} A_t^j \lambda_t^j \bar{\nu}^j dt - \frac{\partial f_t^j}{\partial A_t^j} A_t^j \lambda_t^m \bar{\nu}^m dt, \end{aligned} \tag{B.1}$$

where

$$\begin{aligned} \mu_{f,t}^j &= \frac{\partial f_t^j}{\partial A_t^j} \frac{A_t^j}{f_t^j} (\mu_t - q) + \frac{\partial f_t^j}{\partial V_t} \frac{\kappa(\theta - V_t)}{f_t^j} \\ &+ \frac{1}{2} \frac{\partial^2 f_t^j}{\left(\partial A_t^j\right)^2} \frac{(A_t^j)^2}{f_t^j} \left(\sigma_j^2 + V_t\right) + \frac{1}{2} \frac{\partial^2 f_t^j}{(\partial V_t)^2} \frac{\delta^2 V_t}{f_t^j} \\ &+ \frac{\partial^2 f_t^j}{\partial A_t^j \partial V_t} \frac{A_t^j \rho \delta V_t}{f_t^j}. \end{aligned} \tag{B.2}$$

The $\mathbb{P}$-dynamics above, combined with the SDF defined in equation (4), imply that, in the absence of arbitrage opportunities, the dynamics of the corporate claim or derivative f under $\mathbb{Q}$ are

$$\begin{aligned} df_t^j &= \mu_{f,t}^{j,\mathbb{Q}} f_t^j dt + \frac{\partial f_t^j}{\partial A_t^j} A_t^j \sigma_j dW_t^j + \frac{\partial f_t^j}{\partial A_t^j} A_t^j \sqrt{V_t} dW_t^{A,\mathbb{Q}} + \frac{\partial f_t^j}{\partial V_t} \delta \sqrt{V_t} dW_t^{V,\mathbb{Q}} \\ &+ dJ_t^{j,f} + dJ_t^{m,f,\mathbb{Q}} - \frac{\partial f_t^j}{\partial A_t^j} A_t^j \lambda_t^j \bar{\nu}^j dt - \frac{\partial f_t^j}{\partial A_t^j} A_t^j \lambda_t^m \bar{\nu}^m dt, \end{aligned} \tag{B.3}$$

where

$$dJ_t^{m,f,\mathbb{Q}} = \left(f(A_t^j e^{\tilde{Z}_t^{m,\mathbb{Q}}}, V_t) - f_t^j\right) dN_t^{m,\mathbb{Q}},$$

and where

$$\begin{aligned}
\mu_{f,t}^{j,\mathbb{Q}} &= \frac{\partial f_t^j}{\partial A_t^j}\frac{A_t^j}{f_t^j}(r-q) + \frac{\partial f_t^j}{\partial V_t}\frac{\kappa^{\mathbb{Q}}(\theta^{\mathbb{Q}} - V_t)}{f_t^j} \\
&+ \frac{1}{2}\frac{\partial^2 f_t^j}{\left(\partial A_t^j\right)^2}\frac{(A_t^j)^2}{f_t^j}\left(\sigma_j^2 + V_t\right) + \frac{1}{2}\frac{\partial^2 f_t^j}{(\partial V_t)^2}\frac{\delta^2 V_t}{f_t^j} \\
&+ \frac{\partial^2 f_t^j}{\partial A_t^j \partial V_t}\frac{A_t^j \rho\delta V_t}{f_t^j}. \qquad \text{(B.4)}
\end{aligned}$$

Absence of arbitrage implies that under the risk-neutral measure, we must have

$$\begin{aligned}
\mathbb{E}_t^{\mathbb{Q}}\left[\frac{df_t^j}{f_t^j}\right] &= (r-q)dt \\
&= \mu_{f,t}^{j,\mathbb{Q}}dt + \frac{\mathbb{E}_t\left[dJ_t^{j,f}\right]}{f_t^j} - \frac{\mathbb{E}_t^{\mathbb{Q}}\left[dJ_t^{m,f}\right]}{f_t^j} - \frac{\partial f_t^j}{\partial A_t^j}\frac{A_t^j}{f_t^j}\lambda_t^j\bar{\nu}^j dt - \frac{\partial f_t^j}{\partial A_t^j}\frac{A_t^j}{f_t^j}\lambda_t^m\bar{\nu}^m dt.
\end{aligned}$$

B.2 Model implications for indices and index derivative dynamics

In this appendix, we first derive the dynamics and moments of a generic index consisting of any given corporate securities. We then extend the results to express the dynamics and moments of any derivative written on such index.

Index dynamics

Consider an index I consisting of an equally weighted representation of individual constituents

$$I(A_t^1, \ldots, A_t^N, V_t) = \frac{1}{N}\sum_{j=1}^{N} f(A_t^j, V_t),$$

where f can be a firm's stock price, CDS spread, CDS up-front fee or any other claim written on its assets. Given the dynamics of f in (B.1), the $\mathbb{P}$-dynamics of the index is given by

$$\begin{aligned} dI_t &= \left(\frac{1}{N}\sum_{j=1}^{N}\mu_{f,t}^{j}f_t^j\right)dt + \left(\frac{1}{N}\sum_{j=1}^{N}\frac{\partial f_t^j}{\partial A_t^j}A_t^j\sigma_j dW_t^j\right) + \left(\frac{1}{N}\sum_{j=1}^{N}\frac{\partial f_t^j}{\partial A_t^j}A_t^j\right)\sqrt{V_t}dW_t^A \\ &+ \left(\frac{1}{N}\sum_{j=1}^{N}\frac{\partial f_t^j}{\partial V_t}\right)\delta\sqrt{V_t}dW_t^V + dJ_t^{m,f} - \left(\frac{1}{N}\sum_{j=1}^{N}\frac{\partial f_t^j}{\partial A_t^j}A_t^j\right)\lambda_t^m\bar{\nu}^m dt \\ &+ \left(\frac{1}{N}\sum_{j=1}^{N}dJ_t^{j,f}\right) - \left(\frac{1}{N}\sum_{j=1}^{N}\frac{\partial f_t^j}{\partial A_t^j}A_t^j\lambda^j\bar{\nu}^j\right)dt. \end{aligned} \tag{B.5}$$

A few things need to be noted. First, taking a very large portfolio ($N \to \infty$), by the properties of (idiosyncratic) Brownian motion, the law of large numbers implies that:

$$\lim_{N\to\infty}\frac{1}{N}\sum_{j=1}^{N}\frac{\partial f_t^j}{\partial A_t^j}A_t^j\sigma_j dW_t^j \to 0.$$

Furthermore, recall that

$$dJ_t^{j,f} = \left(f(A_t^j e^{\tilde{Z}_t^j}, V_t) - f_t^j\right)dN_t^j.$$

In our framework, one consequence of homogeneity assumption about firms' dynamics is that all firms share the same idiosyncratic structural parameters such as diffusive volatility (σ_j) and jump intensity (λ_j). Because of this, in the limit, when $N \to \infty$, we have

$$\lim_{N\to\infty}\frac{1}{N}\sum_{j=1}^{N}dJ_t^{j,f} \to \mathbb{E}_t\left[f(A_t^j e^{\tilde{Z}_t^j}, V_t) - f_t^j\right]\lambda^j dt \equiv \bar{J}_t^{j,f}\lambda^j dt.$$

The previous results implies that the dynamics (B.5) of an infinitely large index simplifies to

$$\begin{aligned} dI_t &= \left(\frac{1}{N}\sum_{j=1}^{N}\mu_{f,t}^{j}f_t^j\right)dt + \bar{J}_t^{j,f}\lambda^j dt + \left(\frac{1}{N}\sum_{j=1}^{N}\frac{\partial f_t^j}{\partial A_t^j}A_t^j\right)\sqrt{V_t}dW_t^A \\ &+ \left(\frac{1}{N}\sum_{j=1}^{N}\frac{\partial f_t^j}{\partial V_t}\right)\delta\sqrt{V_t}dW_t^V + dJ_t^{m,f} \\ &- \left(\frac{1}{N}\sum_{j=1}^{N}\frac{\partial f_t^j}{\partial A_t^j}A_t^j\right)\lambda_t^m\bar{\nu}^m dt \\ &- \left(\frac{1}{N}\sum_{j=1}^{N}\frac{\partial f_t^j}{\partial A_t^j}A_t^j\lambda^j\bar{\nu}^j dt\right). \end{aligned} \tag{B.6}$$

The second implication of homogeneity assumption about firms' dynamics is that firms are ex-ante homogeneous, that is, $A_t^j = A_t^r$ for all j at time t but may differ ex-post due to different idiosyncratic shocks.[33] Imposing the homogeneity assumption in (B.6) implies that $I_t = \frac{1}{N}\sum_{j=1}^{N} f(A_t^r, V_t) = f(A_t^r, V_t)$. We also have

$$\begin{gathered} \frac{1}{N}\sum_{j=1}^{N}\mu_{f,t}^{j}f_t^j = \mu_{f,t}^{r}f_t^r = \mu_{I,t}^{r}I_t \\ \bar{J}_t^{j,f} = \bar{J}_t^{r,f} = \bar{J}_t^{r,I} \\ \frac{1}{N}\sum_{j=1}^{N}\frac{\partial f_t^j}{\partial A_t^j}A_t^j = \frac{\partial f_t^r}{\partial A_t^r}A_t^r = \frac{\partial I_t}{\partial A_t^r}A_t^r \\ \frac{1}{N}\sum_{j=1}^{N}\frac{\partial f_t^j}{\partial V_t} = \frac{\partial f_t^r}{\partial V_t} = \frac{\partial I_t}{\partial V_t} \\ \frac{1}{N}\sum_{j=1}^{N}\left(\frac{\partial f_t^j}{\partial A_t^j}A_t^j\lambda^j\bar{\nu}^j\right) = \frac{\partial f_t^r}{\partial A_t^r}A_t^r\lambda^j\bar{\nu}^j = \frac{\partial I_t}{\partial A_t^r}A_t^r\lambda^j\bar{\nu}^j, \end{gathered}$$

where $\bar{J}_t^{r,I} = \mathbb{E}_t\left[I(A_t^r e^{\tilde{Z}_t^j}, V_t) - I_t\right]$. Moreover, $dJ_t^{m,I} = \left(I(A_t^r e^{\tilde{Z}_t^m}, V_t) - I_t\right)dN_t^m$ and from (B.2)

[33] Another way to look at our homogeneity assumption is from the index point of view. More precisely, assuming that firms are ex-ante homogeneous is equivalent to assume that the index is continuously re-balanced to be composed solely of firms for which $A_t^j = A_t^r$.

we get

$$\begin{aligned}\mu^r_{I,t} &= \frac{\partial I_t}{\partial A^r_t}\frac{A^r_t}{I_t}(\mu_t - q) + \frac{\partial I_t}{\partial V_t}\frac{\kappa(\theta - V_t)}{I_t} \\ &+ \frac{1}{2}\frac{\partial^2 I_t}{(\partial A^r_t)^2}\frac{(A^r_t)^2}{I_t}\left(\sigma_j^2 + V_t\right) + \frac{1}{2}\frac{\partial^2 I_t}{(\partial V_t)^2}\frac{\delta^2 V_t}{I_t} \\ &+ \frac{\partial^2 I_t}{\partial A^r_t \partial V_t}\frac{A^r_t \rho\delta V_t}{I_t}.\end{aligned}$$

Plugging these results back into (B.6) implies the following $\mathbb{P}$-dynamics for the index:

$$\frac{dI_t}{I_t} = \bar{\mu}_{I,t}dt + \frac{\partial I_t}{\partial A^r_t}\frac{A^r_t}{I_t}\sqrt{V_t}dW^A_t + \frac{\partial I_t}{\partial V_t}\frac{\delta}{I_t}\sqrt{V_t}dW^V_t + \frac{1}{I_t}dJ^{m,I}_t, \tag{B.7}$$

where $\bar{\mu}_{I,t} \equiv \mu^r_{I,t} + \frac{\bar{J}^{r,I}_t}{I_t}\lambda^j - \frac{\partial I_t}{\partial A^r_t}\frac{A^r_t}{I_t}\left(\lambda^j\bar{\nu}^j + \lambda^m_t\bar{\nu}^m\right)$. It is worth noting that although the initial level of the index is equal to that of the representative firm security $f(A^r_t, V_t)$, their dynamics differ in the sense that those of the index are free of idiosyncratic shocks while the dynamics of the latter are not.[34]

The $\mathbb{P}$-dynamics (B.7) combined with the risk-neutralization of systematic risks implies the following $\mathbb{Q}$-dynamics for the index:

$$\frac{dI_t}{I_t} = \bar{\mu}^{\mathbb{Q}}_{I,t}dt + \frac{\partial I_t}{\partial A^r_t}\frac{A^r_t}{I_t}\sqrt{V_t}dW^{A,\mathbb{Q}}_t + \frac{\partial I_t}{\partial V_t}\frac{\delta}{I_t}\sqrt{V_t}dW^{V,\mathbb{Q}}_t + \frac{1}{I_t}dJ^{m,I,\mathbb{Q}}_t, \tag{B.8}$$

where $\bar{\mu}^{\mathbb{Q}}_{I,t} \equiv \mu^{r,\mathbb{Q}}_{I,t} + \frac{\bar{J}^{r,I}_t}{I_t}\lambda^j - \frac{\partial I_t}{\partial A^r_t}\frac{A^r_t}{I_t}\left(\lambda^j\bar{\nu}^j + \lambda^m_t\bar{\nu}^m\right)$ and $dJ^{m,I,\mathbb{Q}}_t = \left(I(A^r_t e^{\tilde{Z}^{m,\mathbb{Q}}_t}, V_t) - I_t\right)dN^{m,\mathbb{Q}}_t$, and

[34] Similarly, while in level, we have $A^m_t = A^r_t$ for a large portfolio A^m_t constituted of individual firm unlevered assets A^r_t, the dynamics of A^r_t is function of idiosyncratic risks while dA^m_t is not because of the effect of diversification.

where

$$\begin{aligned}\mu_{I,t}^{r,\mathbb{Q}} &= \frac{\partial I_t}{\partial A_t^r}\frac{A_t^r}{I_t}(r-q) + \frac{\partial I_t}{\partial V_t}\frac{\kappa^{\mathbb{Q}}(\theta^{\mathbb{Q}}-V_t)}{I_t} \\ &+ \frac{1}{2}\frac{\partial^2 I_t}{\left(\partial A_t^j\right)^2}\frac{(A_t^r)^2}{I_t}\left(\sigma_j^2+V_t\right) + \frac{1}{2}\frac{\partial^2 I_t}{(\partial V_t)^2}\frac{\delta^2 V_t}{f_t^j} \\ &+ \frac{\partial^2 I_t}{\partial A_t^r \partial V_t}\frac{A_t^r \rho \delta V_t}{I_t}. \end{aligned} \tag{B.9}$$

From equations (B.7)-(B.10), we can now derive the index expected returns under $\mathbb{P}$ and $\mathbb{Q}$ as well as its conditional variance. The expected returns under the physical and risk-neutral probability measures are

$$\begin{aligned}\mathbb{E}_t\left[\frac{dI_t}{I_t}\right] &= \bar{\mu}_{I,t}dt + \frac{\mathbb{E}_t\left[dJ_t^{m,I}\right]}{I_t} \\ \mathbb{E}_t^{\mathbb{Q}}\left[\frac{dI_t}{I_t}\right] &= \bar{\mu}_{I,t}^{\mathbb{Q}}dt + \frac{\mathbb{E}_t^{\mathbb{Q}}\left[dJ_t^{m,I,\mathbb{Q}}\right]}{I_t},\end{aligned}$$

respectively. So, we can write the index return risk premium as

$$\begin{aligned}\mathbb{E}_t\left[\frac{dI_t}{I_t}\right] - E_t^{\mathbb{Q}}\left[\frac{dI_t}{I_t}\right] &= \left(\mu_{I,t}^r - \mu_{I,t}^{r,\mathbb{Q}}\right)dt + \frac{1}{I_t}\left(\mathbb{E}_t\left[dJ_t^{m,I}\right] - \mathbb{E}_t^{\mathbb{Q}}\left[dJ_t^{m,I,\mathbb{Q}}\right]\right) \\ &= \frac{\partial I_t}{\partial A_t^r}\frac{A_t^r}{I_t}(\mu_t - r)\,dt + \frac{\partial I_t}{\partial V_t}\frac{\delta\xi_V V_t}{I_t}dt + \frac{1}{I_t}\left(\mathbb{E}_t\left[dJ_t^{m,I}\right] - \mathbb{E}_t^{\mathbb{Q}}\left[dJ_t^{m,I,\mathbb{Q}}\right]\right).\end{aligned} \tag{B.10}$$

The instantaneous physical and risk-neutral index return variance $\sigma_{I,t}^2$ and $\sigma_{I,t}^{2,\mathbb{Q}}$ can be expressed

as

$$\begin{aligned}
\sigma_{I,t}^2 &= \left[\left(\frac{A_t^r}{I_t}\frac{\partial I_t}{\partial A_t^r}\right)^2 + \left(\frac{\delta}{I_t}\frac{\partial I_t}{\partial V_t}\right)^2 + 2\rho\delta\frac{A_t^r}{(I_t)^2}\frac{\partial I_t}{\partial A_t^r}\frac{\partial I_t}{\partial V_t}\right]V_t + \lambda_t^m\mathbb{E}_t\left[\frac{I(A_t^r e^{\tilde{Z}_t^m}, V_t)}{I_t} - 1\right]^2 \\
\sigma_{I,t}^{2,\mathbb{Q}} &= \left[\left(\frac{A_t^r}{I_t}\frac{\partial I_t}{\partial A_t^r}\right)^2 + \left(\frac{\delta}{I_t}\frac{\partial I_t}{\partial V_t}\right)^2 + 2\rho\delta\frac{A_t^r}{(f_t^r)^2}\frac{\partial I_t}{\partial A_t^r}\frac{\partial I_t}{\partial V_t}\right]V_t + \lambda_t^{m,\mathbb{Q}}\mathbb{E}_t^{\mathbb{Q}}\left[\frac{I(A_t^r e^{\tilde{Z}_t^{m,\mathbb{Q}}}, V_t)}{I_t} - 1\right]^2.
\end{aligned} \tag{B.11}$$

Index derivative dynamics

The results presented in equations (B.7), (B.10), and (B.11) can be easily extended to any derivatives O written on the index whether it corresponds to a call, $c(I_t, K, T)$, or a put, $p(I_t, K, T)$, with respective payoffs $e^{-rT}\mathbb{E}_t^{\mathbb{Q}}\left[max(I_{t+T} - K, 0)\right]$ or $e^{-rT}\mathbb{E}_t^{\mathbb{Q}}\left[max(K - I_{t+T}, 0)\right]$.

To see why, simply note that the state variables impacting the index valuations (i.e., A_t^r and V_t in our case after imposing firm homogeneity) are the same that would impact the pricing of any derivative. In other words, if $I_t = f(A_t^r, V_t)$ then we must have $O(A_t^r, V_t)$. Denoting $O_t \equiv O(A_t^r, V_t)$, we thus get

$$\begin{aligned}
\mathbb{E}_t\left[\frac{dO_t}{O_t}\right] - E_t^{\mathbb{Q}}\left[\frac{dO_t}{O_t}\right] &= \frac{\partial O_t}{\partial A_t^r}\frac{A_t^r}{O_t}\left(\mu_t - r\right)dt + \frac{\partial O_t}{\partial V_t}\frac{\delta\xi_V V_t}{O_t}dt + \frac{1}{O_t}\left(\mathbb{E}_t\left[dJ_t^{m,O}\right] - \mathbb{E}_t^{\mathbb{Q}}\left[dJ_t^{m,O,\mathbb{Q}}\right]\right). \\
\sigma_{O,t}^2 &= \left[\left(\frac{A_t^r}{O_t}\frac{\partial O_t}{\partial A_t^r}\right)^2 + \left(\frac{\delta}{O_t}\frac{\partial O_t}{\partial V_t}\right)^2 + 2\rho\delta\frac{A_t^r}{(O_t)^2}\frac{\partial O_t}{\partial A_t^r}\frac{\partial O_t}{\partial V_t}\right]V_t + \lambda_t^m\mathbb{E}_t\left[\frac{O(A_t^r e^{\tilde{Z}_t^m}, V_t)}{O_t} - 1\right]^2 \\
\sigma_{O,t}^{2,\mathbb{Q}} &= \left[\left(\frac{A_t^r}{O_t}\frac{\partial O_t}{\partial A_t^r}\right)^2 + \left(\frac{\delta}{O_t}\frac{\partial O_t}{\partial V_t}\right)^2 + 2\rho\delta\frac{A_t^r}{(O_t)^2}\frac{\partial O_t}{\partial A_t^r}\frac{\partial O_t}{\partial V_t}\right]V_t + \lambda_t^{m,\mathbb{Q}}\mathbb{E}_t^{\mathbb{Q}}\left[\frac{O(A_t^r e^{\tilde{Z}_t^{m,\mathbb{Q}}}, V_t)}{O_t} - 1\right]^2,
\end{aligned} \tag{B.12}$$

where

$$\begin{aligned}
dJ_t^{m,O} &= \left(O(A_t^r e^{\tilde{Z}_t^m}, V_t) - O_t\right)dN_t^m \\
dJ_t^{m,O,\mathbb{Q}} &= \left(O(A_t^r e^{\tilde{Z}_t^{m,\mathbb{Q}}}, V_t) - O_t\right)dN_t^{m,\mathbb{Q}},
\end{aligned}$$

which completes the proof.

C Model Estimation

This Appendix provides details about the estimation of the model. We first present the conditional log-likelihood used for estimating structural parameters. We then describe the estimation of model-implied measures such as 5-year CDX spread or conditional equity index volatility that are used as inputs to the estimation.

C.1 Maximizing model log-likelihood

We estimate Θ by maximum likelihood. The log-likelihood function is given by

$$\log \mathcal{L}(\Theta) = \sum_{t=2}^{T} \log \mathbb{P}\left(Y_t \mid Y_{t-1}; \Theta\right). \tag{C.1}$$

For ease of exposition, we split Y_t into two vectors: $Y_t^a = \left\{S_{5,t}^{\text{CDX}}, \sigma_t^{\text{SPX}}\right\}$ which denotes the variables that are assumed to be accurately observed and $Y_t^b = \left\{S_{3,t}^{\text{CDX}}, S_{7,t}^{\text{CDX}}, S_{10,t}^{\text{CDX}}\right\}$, the vector of the remaining CDX spreads. By Bayes' rule, the transition probability of Y_t can be expressed as

$$\mathbb{P}\left(Y_t \mid Y_{t-1}; \Theta\right) \;=\; \mathbb{P}\left(Y_t^b \mid Y_t^a; \Theta\right) \times \mathbb{P}\left(Y_t^a \mid Y_{t-1}^a; \Theta\right). \tag{C.2}$$

We compute the two conditional probabilities in equation (C.2) individually. First, the probability of observing Y_t^b conditional on Y_t^a is equivalent to observing the measurement errors $e_{T,t}$ in equation (17). This implies that the first conditional probability $\mathbb{P}\left(Y_t^b \mid Y_t^a; \Theta\right)$ is Gaussian and is given by

$$\mathbb{P}\left(Y_t^b \mid Y_t^a; \Theta\right) = \prod_{T=3,7,10} \frac{1}{\sigma_e\sqrt{2\pi}} e^{-\frac{e_{T,t}^2}{2\sigma_e^2}}. \tag{C.3}$$

Second, it is worth noting that observing Y_t^a is equivalent to observing (A_t^r, V_t) or even (a_t^r, V_t)

where $a_t^r \equiv \log(A_t^r)$. This result follows from the equality in equation (16) and the existence of the one-to-one mapping between the two state variables (or (a_t^r, V_t)) and $S_{5,t}^{\text{CDX}}$ and σ_t^{SPX}. Hence, the second conditional probability $\mathbb{P}\left(Y_t^a \mid Y_{t-1}^a; \Theta\right)$ is equal to the transition probability of (a_t^r, V_t) divided by the absolute value of the Jacobian determinant of the mapping $(a_t^r, V_t) \mapsto Y_t^a$. We have

$$\mathbb{P}\left(Y_t^a \mid Y_{t-1}^a; \Theta\right) = \frac{1}{|\det(J_t)|}\mathbb{P}\left(a_t^r, V_t \mid a_{t-1}^r, V_{t-1}; \Theta\right), \tag{C.4}$$

where[35]

$$J_t = \begin{bmatrix} \frac{\partial S_{5,t}^{\text{CDX}}}{\partial a_t^r} & \frac{\partial S_{5,t}^{\text{CDX}}}{\partial V_t} \\ \frac{\partial \sigma_t^{\text{SPX}}}{\partial a_t^r} & \frac{\partial \sigma_t^{\text{SPX}}}{\partial V_t} \end{bmatrix}. \tag{C.5}$$

In equation (C.4), the conditional probability can further be decomposed into

$$\mathbb{P}\left(a_t^r, V_t \mid a_{t-1}^r, V_{t-1}; \Theta\right) = \mathbb{P}\left(a_t^r \mid V_t, a_{t-1}^r, V_{t-1}; \Theta\right) \times \mathbb{P}\left(V_t \mid V_{t-1}; \Theta\right). \tag{C.6}$$

In the previous equation, $\mathbb{P}\left(V_t \mid V_{t-1}; \Theta\right)$ corresponds to the Bessel density function of observing V_t conditional on V_{t-1} which is available in closed-form. We are thus left with the estimation of $\mathbb{P}\left(a_t^r \mid V_t, a_{t-1}^r, V_{t-1}; \Theta\right)$.

To estimate $\mathbb{P}\left(a_t^r \mid V_t, a_{t-1}^r, V_{t-1}; \Theta\right)$, we adopt the following strategy. We first need to express the (discretized) dynamics of $a_t^r = \log(A_t^r)$. To this end, we apply an Euler-discretization scheme to the continuous-time dynamics of a_t^r. We get:

$$\begin{aligned} a_t^r &= a_{t-1}^r + (\mu_{t-1} - q)\Delta t + \sqrt{V_{t-1}}\Delta W_t^A + \Delta J_t^m - \lambda_t^m \bar{\nu}^m \Delta t \\ &\quad + \sigma_j \Delta W_t^j + \Delta J_t^j - \lambda^j \bar{\nu}^j \Delta t, \end{aligned} \tag{C.7}$$

where $\Delta W_t^A = \rho \Delta W_t^V + \sqrt{1-\rho^2}\Delta W_t^{A\perp V}$ is normally distributed $N(0, \Delta t)$ and $\Delta J_t^k \equiv \sum_{N_{t-1}^k}^{N_t^k} \tilde{Z}_t^k$ with $\tilde{Z}_t^k \sim N(z_k, \gamma_k^2)$ for $k = j, m$. Thus, ΔJ_t^k denotes the discretized jump process and N_t^k counts

[35] We refer to Appendix C.2 for details about the computation of J_t.

the total number of jumps that have occurred up to time t. In the above equation, recall that

$$\mu_{t-1} = r + \left(\sqrt{1-\rho^2}\xi_A + \rho\xi_V\right) V_{t-1} + \lambda^m_{t-1}\mathbb{E}_{t-1}\left[\tilde{\nu}^m_{t-1}\right] - \lambda^m_{t-1}\mathbb{E}^{\mathbb{Q}}_{t-1}\left[\tilde{\nu}^{m,\mathbb{Q}}_{t-1}\right].$$

Consequently, μ_{t-1} is only function of V_{t-1} and the structural parameters. Conditionally on observing V_t, V_{t-1}, and a^r_{t-1}, the distribution of a^r_t can be defined by

$$a^r_t = F_t + \sqrt{V_{t-1}}\sqrt{1-\rho^2}\Delta W^{A\perp V}_t + \Delta J^m_t + \sigma_j \Delta W^j_t + \Delta J^j_t, \tag{C.8}$$

where $\Delta W^{A\perp V}_t$, ΔJ^m_t, ΔW^j_t , and ΔJ^j_t capture the remaining uncertainty in a^r_t after conditioning, and

$$F_t = a^r_{t-1} + (\mu_{t-1} - q)\,\Delta t + \sqrt{V_{t-1}}\rho\Delta W^V_t - \lambda^m_t\bar{\nu}^m\Delta t - \lambda^j\bar{\nu}^j\Delta t,$$

is the conditional expectation of a^r_t given V_t, a^r_{t-1}, V_{t-1} with

$$\Delta W^V_t = \frac{V_t - V_{t-1} - \kappa(\theta - V_{t-1})\Delta t}{\delta\sqrt{V_{t-1}}},$$

which is known after conditioning.

We have now all the required ingredients to derive an estimate of $\mathbb{P}\left(a^r_t \mid V_t, a^r_{t-1}, V_{t-1}; \Theta\right)$. To achieve this objective, first note that

$$\begin{aligned} &\mathbb{P}\left(a^r_t \mid V_t, a^r_{t-1}, V_{t-1}; \Theta\right) \\ = &\sum_{u_j=0}^{U_j}\sum_{u_m=0}^{U_m} \mathbb{P}\left(a^r_t \mid N^m_t = u_m, N^j_t = u_j, V_t, a^r_{t-1}, V_{t-1}; \Theta\right)\mathbb{P}\left(N^m_t = u_m \mid V_{t-1}; \Theta\right)\mathbb{P}\left(N^j_t = u_j \mid V_{t-1}; \Theta\right), \end{aligned} \tag{C.9}$$

where

$$\mathbb{P}\left(a^r_t \mid N^m_t = u_m, N^j_t = u_j, V_t, a^r_{t-1}, V_{t-1}; \Theta\right) \equiv \frac{1}{\sigma_t(a^r)\sqrt{2\pi}} e^{-\frac{(a^r_t - \mu_t(a^r))^2}{2\sigma^2_t(a^r)}}, \tag{C.10}$$

with

$$\begin{aligned}\mu_t(a^r) &\equiv \mathbb{E}\left[a_t^r \mid N_t^m = u_m, N_t^j = u_j, V_t, a_{t-1}^r, V_{t-1}; \Theta\right] \\ &= F_t + (u_m z_m)\Delta t + (u_j z_j)\Delta t,\end{aligned}$$

and with

$$\begin{aligned}\sigma_t^2(a^r) &\equiv Var\left[a_t^r \mid N_t^m = u_m, N_t^j = u_j, V_t, a_{t-1}^r, V_{t-1}; \Theta\right] \\ &= V_{t-1}(1-\rho^2)\Delta t + \sigma_j^2 \Delta t + u_m(z_m^2 + \gamma_m^2)\Delta t + u_j(z_j^2 + \gamma_j^2)\Delta t.\end{aligned}$$

Moreover, we have

$$\mathbb{P}\left(N_t^m = u_m \mid V_{t-1}; \Theta\right) = \frac{(V_{t-1}\eta_m \Delta t)^{u_m}}{u_m!} e^{-V_{t-1}\eta_m \Delta t}, \tag{C.11}$$

and

$$\mathbb{P}\left(N_t^j = u_j \mid V_{t-1}; \Theta\right) = \frac{(\lambda_j \Delta t)^{u_j}}{u_j!} e^{-\lambda_j \Delta t}. \tag{C.12}$$

To estimate $\mathbb{P}\left(a_t^r \mid V_t, a_{t-1}^r, V_{t-1}; \Theta\right)$ in equation (C.9), we set $U_m = 10$ and $U_j = 1$ and multiply equations (C.11), (C.11), and (C.12) together.[36]

Then, finally, we obtain our maximum likelihood estimates by searching for the set of model parameters Θ that maximizes the log-likelihood function $\log \mathcal{L}(\Theta)$ in equation (C.1).

C.2 Estimation details on $P_D(A_t^j, V_t)$, $G(A_t^j, V_t, T)$, $S_{T,t}^{\mathbf{CDX}}$, $\sigma_t^{\mathbf{SPX}}$, and J_t

Recall that in our estimation methodology, we need to compute the T-year CDX spread ($S_{T,t}^{\text{CDX}}$) and the conditional SPX return volatility (σ_t^{SPX}) as well as the Jacobian matrix J_t to estimate

[36]Note that the truncations chosen are not restrictive given our daily estimation strategy combined with the relatively low intensity of jumps (1 per year on average for systematic jumps and 1 every 10 years for idiosyncratic jumps).

model parameters and filter (A_t^r, V_t). Given model dynamics and our homogeneity assumption, we have the following variable definitions. First, $S_{T,t}^{\text{CDX}}$ corresponds to $S(A_t^r, V_t, T)$ where $S(A_t^r, V_t, T)$ satisfies equation (11) setting $A_t^j = A_t^r$. Moreover, σ_t^{SPX} is equal to $\sqrt{\sigma_{E,t}^2}$ with $\sigma_{E,t}^2$ satisfies equation (15) in Proposition (1) setting $A_t^j = A_t^r$ and $I(A_t^r, V_t)$ to $E(A_t^r, V_t)$ where $E(A_t^r, V_t)$ is given by equation (10).[37]

The first step toward estimating $S_{T,t}^{\text{CDX}}$ and σ_t^{SPX} for a given pair of A_t^r and V_t and a given set of structural parameters is to estimate the present value of a dollar received at default $P_D(A_t^r, V_t) = \mathbb{E}_t^{\mathbb{Q}}\left[e^{-r(\tau-t)}\right]$ and the cumulative risk-neutral default probability $G(A_t^r, V_t, T) = \mathbb{E}_t^{\mathbb{Q}}\left[1_{\tau \leqslant T}\right]$ over the next T years where τ is the first time at which the representative firm asset value hits the default boundary. On the one hand, equity prices and thus the instantaneous equity index volatility depends on the sensitivity of P_D with respect to the state variables. To estimate these sensitivities and calculate σ_t^{SPX}, we must first estimate P_D. On the other hand, the term-structure of risk-neutral default probability is the required input to estimate the CDX spread at any horizon T.

We now describe the methodology to estimate $\hat{P}_D(\cdot,\cdot)$, $\hat{G}(\cdot,\cdot,T)$, and their partial derivatives for a given set of structural parameters. First, we discretize the state space of the two state variables, A_t^r and V_t.[38] A given combination of the discretized state variables is then used as initial values for our simulation exercise. Specifically, we adopt a daily discretization of the risk-neutral dynamics of assets and systematic variance using an Euler approximation scheme. More precisely, we simulate

$$\begin{aligned}
\log\left(A_t^r\right) &= \log\left(A_{t-1}^r\right) + (r-q)\,\Delta t + \sqrt{V_{t-1}}\Delta W_t^{A,\mathbb{Q}} + \Delta J_t^{m,\mathbb{Q}} - \lambda_t^m \bar{\nu}^m \Delta t \\
&\quad + \sigma_j \Delta W_t^j + \Delta J_t^j - \lambda^j \bar{\nu}^j \Delta t, \\
V_t &= V_{t-1} + \kappa^{\mathbb{Q}}(\theta^{\mathbb{Q}} - V_{t-1})\Delta t + \delta\sqrt{V_{t-1}}\Delta W_t^{V,\mathbb{Q}},
\end{aligned}$$

[37] Note that we omit the dependence of $S_{T,t}^{\text{CDX}}$ and σ_t^{SPX} on the vector of structural parameters Θ for ease of exposition.

[38] More precisely, we adopt a grid composed of 17 nodes for asset value and 11 nodes for spot variances. The lower and upper bounds for asset values are $A_D + 5$ and 100, respectively. The lower and upper bounds for spot systematic variances correspond to $\theta/100$ and $\theta \cdot 10$, respectively. These bounds combined with our Chebyshev polynomial approach define the nodes.

where $\Delta W_t^{A,\mathbb{Q}} = \rho \Delta W_t^{V,\mathbb{Q}} + \sqrt{1-\rho^2}\Delta W_t^{A\perp V,\mathbb{Q}}$, and $\Delta W_t^{V,\mathbb{Q}}$ and $\Delta W_t^{A\perp V,\mathbb{Q}}$ are two independent normally distributed $N(0,\Delta t)$ shocks. For systematic jumps, we have $\Delta J_t^{m,\mathbb{Q}} \equiv \sum_{N_{t-1}^{m,\mathbb{Q}}}^{N_t^{m,\mathbb{Q}}} \tilde{Z}_t^{m,\mathbb{Q}}$ with $\tilde{Z}_t^{m,\mathbb{Q}} \sim N(z_m^{\mathbb{Q}}, \gamma_m^2)$. Thus, $\Delta J_t^{m,\mathbb{Q}}$ denotes the discretized systematic jump process under $\mathbb{Q}$ and $N_t^{m,\mathbb{Q}}$ counts the total number of jumps that have occurred up to time t. Because systematic jump risk is priced, recall that the risk-neutral intensity of systematic jumps is $\lambda_t^{m,\mathbb{Q}}$. For idiosyncratic jumps, we have $\Delta J_t^j \equiv \sum_{N_{t-1}^j}^{N_t^j} \tilde{Z}_t^j$ with $\tilde{Z}_t^j \sim N(z_j, \gamma_j^2)$.

Using these discretized dynamics, the vector of structural parameters, and a given combination of the initial state variables $\{A_0^r, V_0\}$, we simulate firm assets under the risk-neutral measure over 10 years. Using the simulated paths of firm assets, we then estimate $\hat{P}_D(A_0^r, V_0)$ as $\hat{E}_0^{\mathbb{Q}}\left[e^{-r\tau}\right] = \frac{1}{MC}\sum_{n=1}^{MC} e^{-r\tau^n}$, where $\tau^n = \inf\{s \geqslant 0 : A_s^{r,n} \leqslant A_D\}$ and $A_s^{r,n}$ denotes the representative firm's asset value at time s for the simulated path n, A_D represents the default boundary, and MC is the number of Monte-Carlo simulations.[39] In a similar manner, we can compute the term-structure of risk-neutral cumulative default probability and estimate credit default swaps of any given maturity. Based on the simulations, the cumulative risk-neutral default probability over any horizon T is $\hat{G}(A_0^r, V_0, T) = \hat{E}_0^{\mathbb{Q}}\left[1_{\tau \leqslant T}\right] = \frac{1}{MC}\sum_{n=1}^{MC} 1_{\tau^n \leqslant T}$. Once the cumulative risk-neutral default probability is obtained, it becomes straightforward to estimate the corresponding CDX spread, $\hat{S}(A_0^r, V_0, T)$.

We repeat this simulation exercise for each combination of the initial values of the state variables. This gives us an entire cross-section of P_D as a function of the initial states (i.e., the initial combination of state variables used to simulate the representative firm forward). Using the cross-section of P_D and the combination of states, we then estimate the loadings of Chebyshev polynomials for a given vector of parameters by projecting the P_D on the state variables. The estimated Chebyshev loadings provide us with the required (smooth) mapping between P_D and the state variables, that is, $\hat{P}_D(\cdot,\cdot)$. Because Chebyshev polynomials guarantee a smooth mapping between $\hat{P}_D(\cdot,\cdot)$ and $\{A_t^r, V_t\}$, the estimates of the partial derivatives of $\hat{P}_D(\cdot,\cdot)$ with respect to A_t^r, and V_t are then relatively straightforward to compute. We can in the same manner estimate

[39] We use $MC = 1500$ for computational efficiency.

the Chebyshev loadings providing us with the smooth mapping between $\hat{S}(\cdot,\cdot,T)$ and the state variables. At this point, we can estimate the present value of a dollar received at default, CDX spreads, and their respective derivatives with respect to the state variables for any A_t^r and V_t.

From the expression derived for the conditional equity index physical volatility, we see that one needs to compute the required partial derivatives of P_D with respect to the state variables to estimate $\sigma_{E,t}^2$ for any given A_t^r and V_t (i.e., $\Delta_{A,t} = \frac{\partial I_t}{\partial A_t^r}\frac{A_t^r}{I_t}$ and $\Delta_{V,t} = \frac{\partial I_t}{\partial V_t}, \frac{1}{I_t}$ with $I_t = E(A_t^r, V_t)$). Because of the smooth properties of Chebyshev polynomials, computing these partial derivatives is straightforward once the mapping between P_D and the state variables is estimated.

Finally, recall that our estimation strategy requires computing the Jacobian matrix in equation (C.5) which is function of the partial derivatives of $S_{5,t}^{\text{CDX}}$ and σ_t^{SPX} with respect to log-asset value and spot variance. Again, each element of the Jacobian matrix can be backed-out from the estimated Chebyshev coefficients defining the mapping between S and P_D and the two states.

00

D Comparison with Collin-Dufresne, Junge, and Trolle (2021)

We now discuss our results for SPX options and CDX swaptions in light of the contrasting results in Collin-Dufresne, Junge, and Trolle (2021) (CJT). It is worth noting that our assumptions about the representative firm asset dynamics are identical to CJT and the only difference between our respective frameworks lies in the way that the firm's capital structure is modeled. Hence our main goal in this appendix is to understand whether this can drive the differences in findings.

To see if this is the case, we proceed as follows. Using the parameters reported in CJT applied in our model, we seek to replicate their main results. CJT report two sets of parameters. They do not fit $\mathbb{P}$-dynamics and focus on fitting each derivative markets' risk-neutral distribution. We refer to SPX- (resp. CDX-) parameters as the set of structural parameters in CJT obtained when fitting SPX options (resp. CDX swaptions). The main empirical result in CJT is that SPX options are overpriced when using CDX-parameters while CDX swaptions are underpriced when using SPX-parameters.

For this exercise, the values used for distress costs (α), corporate tax rate (ζ), recovery rate (R), risk-free interest rate (r), asset payout rate (q), coupon payment (c), and default boundary (A_D) are the ones reported in Panel A of Table 1.

Next, we need to define the set of structural parameters and the value of the two state variables. We first discuss the structural parameters used. We then discuss the calibration of the two states which is required for generating CDX and SPX implied volatilities. Since all firm contingent claims are priced under the risk-neutral measure, we can directly use the parameter estimates reported in CJT. However, one additional assumption about the price of systematic jump risk must be made. Recall that the $\mathbb{Q}$-dynamics of the aggregate asset risk factor is given by

$$\frac{dA_t^m}{A_t^m} = (r-q)\,dt + \sqrt{V_t}dW_t^{A,\mathbb{Q}} + dJ_t^{m,\mathbb{Q}} - \lambda_t^m \bar{\nu}^m dt,$$

where $\bar{\nu}^m = \mathbb{E}_t\left[\tilde{\nu}_t^m\right]$ and $\mathbb{E}_t\left[dN_t^m\right] = \lambda_t^m dt = \eta_m V_t dt$. Despite the change of measure, the last term in the previous equation is a function of physical jump intensity and physical expected jump size $\tilde{\nu}_t^m$. When changing numeraire and going from the measure $\mathbb{P}$ to $\mathbb{Q}$, the jump compensator $\lambda_t^m \bar{\nu}^m$ is not affected by the change. This implies that one needs an estimate of the price of systematic jump risk ξ_m to fully define the representative asset $\mathbb{Q}$-dynamics. Because CJT do not estimate $\mathbb{P}$-dynamics and prices of risk, they simply use the risk-neutral compensator in the above $\mathbb{Q}$-dynamics. This is equivalent to assume that $\xi_m = 0$ in which case $\mathbb{P}$ and $\mathbb{Q}$ jump dynamics are perfectly equivalent. For comparison purposes, we follow their approach and set $\xi_m = 0$ when using either sets of parameter (SPX- or CDX-parameters) in our framework. This choice avoids making any ad-hoc assumption about the prices of jump risk in order to be consistent with their two sets of structural parameters.[40]

Armed with the two sets of parameters (one for SPX and one for CDX), we are now left with calibrating the two state variables, A_t^r and V_t. To this end, we simply find the pair of values that

[40]Note that the price of systematic jump is function of jump risk and thus implicitly depends on the jump risk distribution estimated. Note that allowing for economically reasonable price of jump risk parameter does not impact the results of our analysis.

Table A.1: Risk-neutral parameters used for the comparison analysis with CJT

	This Paper	CJT SPX	CJT CDX
Mean reversion speed ($\kappa^{\mathbb{Q}}$)	1.2753	1.074	1.751
Long run mean ($\theta^{\mathbb{Q}}$)	1.42%	3.10%	2.47%
Volatility parameter for asset variance (σ)	0.1879	0.2000	0.2000
Correlation between asset value and variance shocks (ρ)	-0.6195	-0.7000	-0.7000
Systematic jump intensity loading ($\eta_m^{\mathbb{Q}}$: $\lambda_t^{m,\mathbb{Q}} = \eta_m^{\mathbb{Q}} V_t$)	168.5643	8.33	63.96
Systematic jump size mean ($z_m^{\mathbb{Q}}$)	-0.0187	-0.171	-0.045
Systematic jump size standard deviation (γ_m)	1.84%	16.00%	16.70%
Idiosyncratic volatility (σ_ϵ)	9.20%	28.00%	21.00%
Idiosyncratic jump intensity (λ_j)	0.5%	0.1%	0.1%
Idiosyncratic jump size mean (z_j)	-0.9902	-5.0000	-5.0000
Idiosyncratic jump size standard deviation (γ_j)	0.0047	0.0000	0.0000

Notes: The table presents the structural parameters characterizing the representative firm unlevered asset risk-neutral dynamics for our study in the column labelled *This Paper* and for CJT's SPX- and CDX-parameters in the two remaining columns. In the table, $\eta_m^{\mathbb{Q}}$ defines the loading of systematic jump intensity on V_t under the probability measure $\mathbb{Q}$. In our set-up, it is equal to $\eta_m^{\mathbb{Q}} = \eta_m e^{\xi_m z^m + \frac{1}{2}(\xi_m)^2 \gamma_m^2}$. For the two sets of CJT parameters, it is directly equal to the value reported in their study. Note the parameters reported for CJT are the ones used to produce the results presented in Table A.2.

Table A.2: Comparison of Model Estimates with Collin-Dufresne et al. (2022)

	This Paper	CJT SPX	CJT CDX
	Panel A: State Variables and Other Metrics		
A_t^r	46.86	112.94	101.54
V_t	0.0093	0.0148	0.0150
L_t	46.11%	19.36%	21.48%
$\sigma_A^{\mathbb{Q}}$	2.93%	15.08%	14.19%
	Panel B: CDX Index Spreads		
5-Year	79.84	79.84	79.84
K	Panel C: S&P 500 Index Implied Volatility		
95%	18.13	18.40	23.12
100%	15.93	15.93	19.52
105%	14.22	14.26	19.09
K	Panel D: CDX Index Implied Volatility		
95%	44.85	33.84	42.54
100%	47.27	36.26	47.38
105%	49.15	38.67	51.79

Notes:

allows to match, for a given set of parameters, the average 5-year CDX spread of 79.84 bps and the 1 month-ATM average implied-volatility by our fitted model. For the set of SPX-parameters (resp. CDX-parameters), we match the average 1 month-ATM SPX (resp. CDX) implied volatility reported in Table 3 (resp. Table 4).

Based on the structural parameters and the state variables, we then generate the 1-month implied-volatilities for CDX swaptions and SPX options. We present the results in Table A.2 and report the parameter estimates for our study, and the SPX- and CDX-parameters in Table A.1. We now discuss the results reported in Table A.2 in more details.

In Panel A, we report the fitted asset value, systematic variance, market leverage as well as the total unlevered asset $\mathbb{Q}$-volatility implied by each parameter set. For our study, the asset value and systematic variance correspond to the time series average of the filtered states. For CJT, they correspond to the one calibrated to match the average 5-year CDX spread of 79.84 basis points and the 1 month-ATM average implied-volatility fitted by our model, either 1 month-ATM average SPX implied-volatility for SPX-parameters or 1 month-ATM average CDX implied-volatility for CDX-parameters. In Panel B, we report the fitted 5-year CDX spreads for each set of parameters. In Panels C and D, we report the fitted implied volatilities.

A few comments are in order. We see that the asset value and systematic variance calibrated for CJT parameters to match 5-year CDS spread and implied-volatilities are quantitatively different from the ones we filter based on our structural parameters (46.86 v.s. 112.94/101.54). The higher asset value calibrated for CJT parameters when applied to our framework is partly explained by the fact that idiosyncratic jumps are larger in CJT than in our study (see Table A.1). Larger negative jumps tend to push away asset value from the default boundary which explains the results obtained for A_t^r in columns 2 and 3. Note that the asset value calibrated for CJT parameters and reported in the table cannot be directly compared to the one presented in their study. In CJT, two debts co-exist and their face values is economically much larger than the default boundary we assume.[41] This explains why we calibrate asset values of 112.94 and 101.54, respectively, but they

[41]The face value of the short-term debt (D_1) is 98.79 and the face value of the long-term debt (D_2) is 659.62.

report an average asset value of 2905.8. However, we can compare the calibrated market leverage and systematic asset variance for their set of parameters in Table A.2 with the one they report.

From columns 2 and 3 in Panel A, the market leverages obtained by fitting the 5-year CDS spread and our model SPX- and CDX-1mth ATM implied volatility using CJT parameters are 15.08% and 14.19%, respectively. These numbers are of the same order of magnitude as the ones we obtained for their 2 parameter sets.[42] By comparing the results in columns 2 and 3 with the ones in column 1, we see that the market leverage differ greatly between the 3 sets of parameters (ours and theirs). This is explained by the differences in fitted asset value as a higher level of asset value calibrated A_t^r for their parameter sets in turn translates into a lower market leverage.

As a result of lower leverage, a higher unlevered asset unconditional total $\mathbb{Q}$-volatility $\sigma_A^{\mathbb{Q}}$ is calibrated by CJT relative to our study (2.93% v.s. 15.08%/14.19%). This is because the level of financial claims volatility, whether they are credit or equity instruments, is positively impacted by the interaction of asset total volatility and leverage. Given the $\sigma_A^{\mathbb{Q}}$ implied by CJT's parameter sets, we see that the level of systematic variance calibrated to fit 5-year CDS spread and our model SPX- and CDX-1mth ATM implied volatility is comparable in magnitude to the average systematic variance reported in CJT (0.0148/0.0150 v.s. 0.0101/0.0185).

We now discuss the main take away from this comparison analysis. From the second column in Panels C and D, we see that SPX parameters combined with calibrated asset value and systematic variance match precisely the level and skew of SPX implied volatilities but fail short on predicting the right level of CDX implied volatilities. From the third column in Panels C and D, we see that CDX parameters combined with calibrated asset value and systematic variance match precisely the level and skew of CDX implied volatilities but overprice SPX implied volatilities.

Altogether, these results suggest that the difference in the firm capital structure modeling between our two studies does not explain the discrepancy between the pricing performances of SPX and CDX option markets.

The total face value of the two debts is thus 758.41 which is an order of magnitude larger than our calibrated default boundary of 19.50.

[42] CJT calibrate a face value-weighted market leverage ($\frac{D_1}{D_1+D2} \cdot l_1 + \frac{D_2}{D_1+D2} \cdot l_2$) of 20.19%.

Hence the remaining difference between our two studies boils down to differences in the estimated parameters.